CHAPTER 4

Simulation and Control of Novel HESS Configuration

Introduction

This chapter focuses on simulating a 40 kWh DC microgrid that integrates photovoltaic (PV) arrays, Ni-MH batteries, EDLCs, and PEM fuel cells using MATLAB/Simulink. The simulation assesses the system's performance under different operational conditions, emphasizing optimizing energy generation, storage, and distribution.

The main objectives are to enhance power flow management, reduce energy losses, and improve system stability. Following the simulation, advanced optimization techniques will be applied further to refine the DC microgrid's performance and overall efficiency.

Figure 4.1 represents the proposed Bipolar 40KWh DC Microgrid Simulation Model. This model represents a standalone hybrid energy management system that integrates photovoltaic (PV) power generation and battery storage to meet load demands in an off-grid setup. The PV system is equipped with MPPT (Maximum Power Point Tracking) to optimize solar energy harvesting. DC-DC converters regulate voltage, while inverters ensure compatibility with DC loads.

A State of Charge (SOC) controller monitors the battery to maintain efficient charging and discharging cycles, ensuring the system's reliability and longevity. The absence of a grid connection emphasizes the system's capability to operate autonomously, relying entirely on renewable energy and battery storage. Breakers and protection circuits ensure safety and fault management, while the modular structure enables scalability for various off-grid energy applications.

Power management for 40KWh DC Microgrid Model

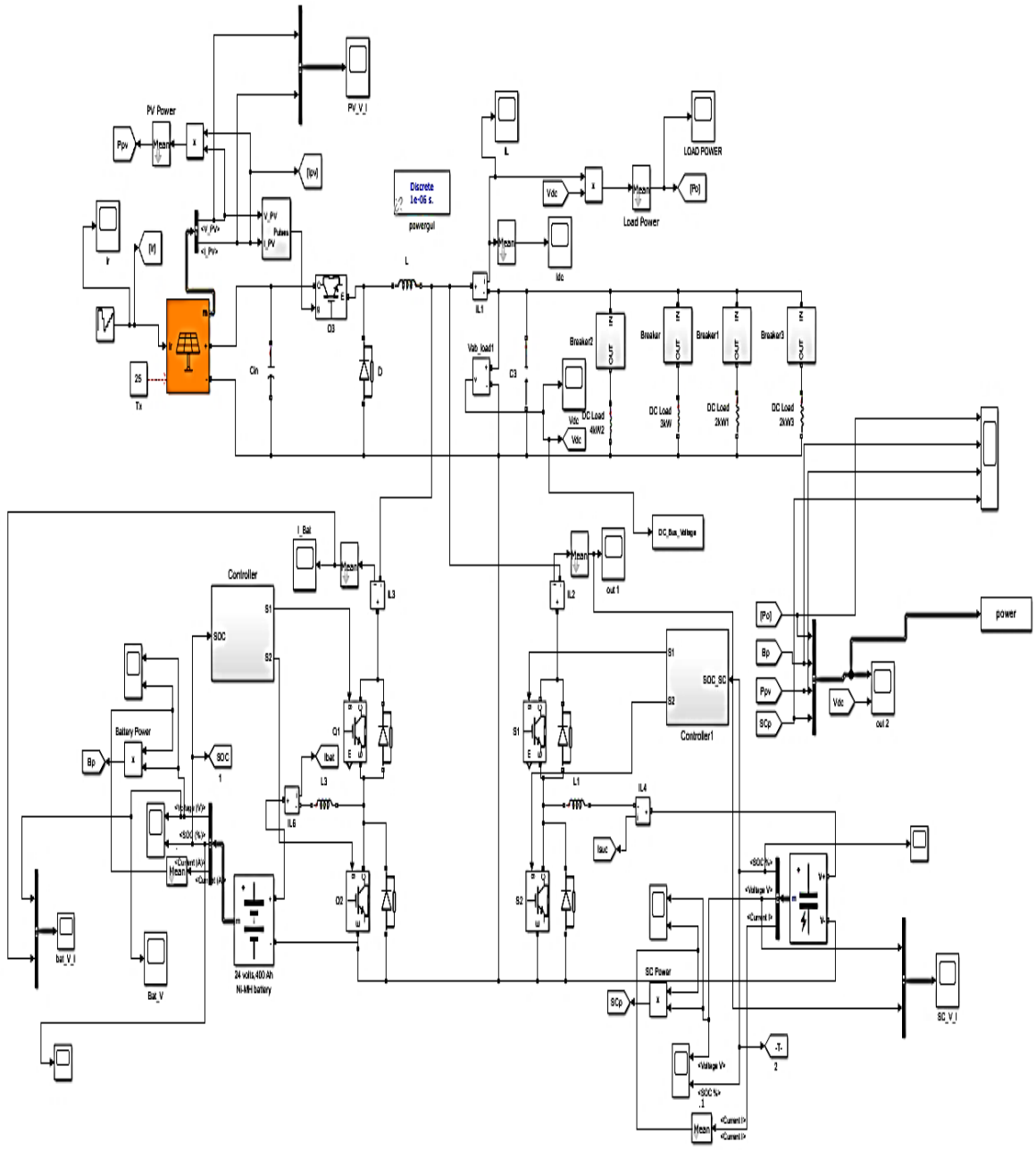

Figure 4. 1 Simulation of DC Microgrid (40 KW,380 V DC)

4.1 Simulation of the Proposed Photovoltaic Array Model

The simulation of the photovoltaic (PV) array model is essential for the DC microgrid system. The model is designed to simulate the operational characteristics of the PV system, including power generation under varying environmental conditions. This simulation is essential for understanding the dynamic performance of the PV array and its integration into the overall DC microgrid architecture.

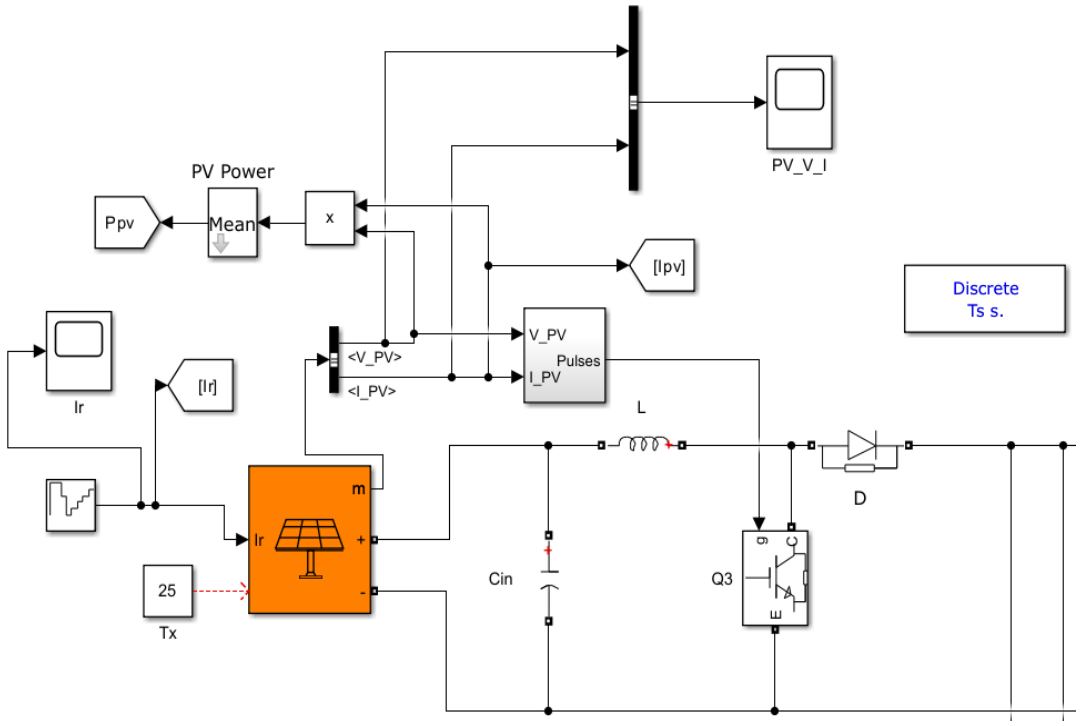

Figure 4. 2 PV Simulation in DC Microgrid

Figure 4.2 illustrates a simulation model for a photovoltaic (PV) system with a DC-DC boost converter, implemented in a discrete-time simulation environment. The PV panel block generates power based on solar irradiance (Ir) and temperature (Tx), producing an output voltage (V_{PV}) and current (I_{PV}). These outputs are fed into a boost converter circuit, comprising an inductor (L), capacitor (Cin), diode (D), and a switching transistor (Q3), which regulates the output to maintain the desired voltage.

The system calculates the PV power (P_{PV}) by multiplying voltage and current, and it uses a feedback control loop to optimize performance. Key monitoring points include the PV voltage, current, and power, visualized in the block labeled (PV_V_I).

The transistor's switching pulses are controlled via a PWM block based on feedback to ensure maximum power transfer. This model is suitable for analyzing the behaviour of PV systems and their integration into DC microgrids.

Table 4. 1 Parameters for the PV Model

Parameters	Range
Open circuit Voltage	48.57 V
Short circuit current	13.70 A
Maximum power	530 W
Voltage at the maximum power point	41.49V
Current at the maximum power point	12.79 A
Service life	12 Year
Series resistance	0.37039 ohm
Shunt resistance	200 ohms
Cells per module	144
Diode ideality factor	0.99739

Table 4.1 presents the key specifications of the Adani Solar Bifacial 530-Watt Solar Panel parameters. These specifications encompass critical electrical and mechanical parameters such as the panel's maximum power output, open circuit voltage, short circuit current, operating voltage at maximum power point (MPP), and current at MPP.

These values are vital for evaluating the panel’s performance under various environmental conditions, optimizing its integration into solar power systems, and ensuring it meets the requirements of high-performance, large-scale solar installations.

4.1.1 Control Strategies in PV Generation

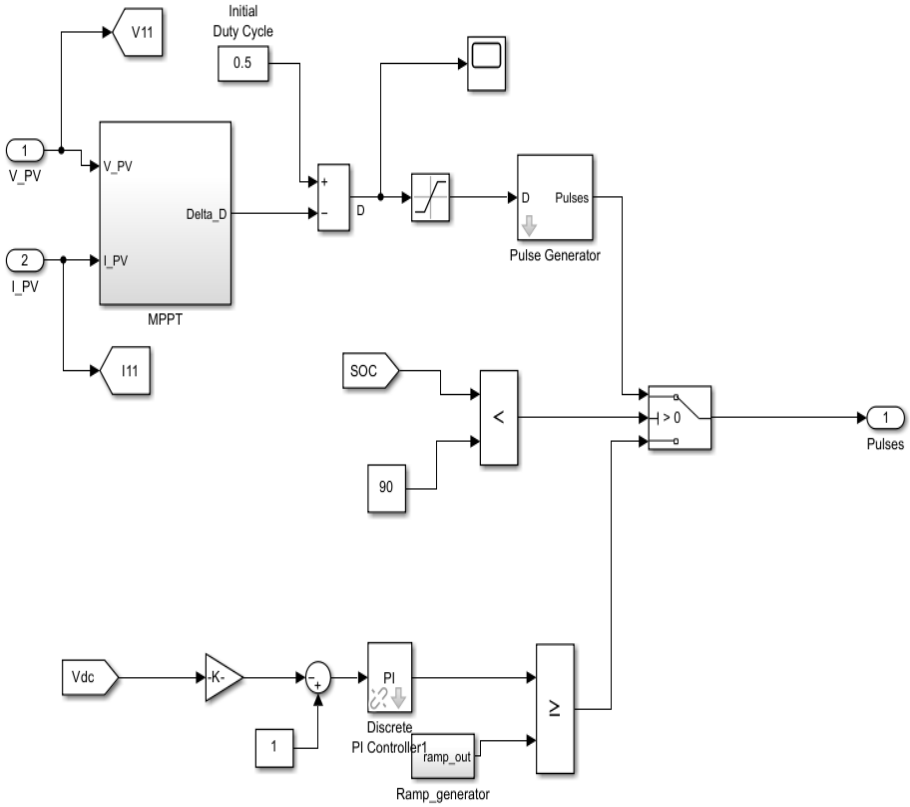

Figure 4. 3 Control Strategies for PV System

Figure 4.3 illustrates an advanced and robust control architecture for a photovoltaic (PV) generation system, incorporating multiple sophisticated techniques to enhance system performance and ensure operational safety and efficiency. This system maintains the DC link voltage, prevents battery overcharging, and mitigates load-shedding issues, ensuring uninterrupted and reliable power delivery. It achieves these objectives by employing three principal mechanisms: Maximum Power Point Tracking (MPPT), State-of-Charge (SOC)-based supervisory control, and a Discrete Proportional-Integral (PI) regulator. These mechanisms work synergistically to form a comprehensive and adaptive control strategy, enabling optimal energy utilization, system stability, and seamless power management under dynamic operating conditions. A detailed analysis of each functional module and its critical role in optimizing operational efficiency and dynamic performance is presented below.

4.1.1.1 Incremental Conductance (INC) algorithm

This section presents the simulation model of the Incremental Conductance (INC) algorithm, a method for maximum power point tracking (MPPT) in photovoltaic (PV) systems. The INC algorithm adjusts the PV array's operating point based on changes in voltage and current, optimizing power extraction under varying conditions. This model highlights its implementation within the DC microgrid to improve energy generation and system integration.

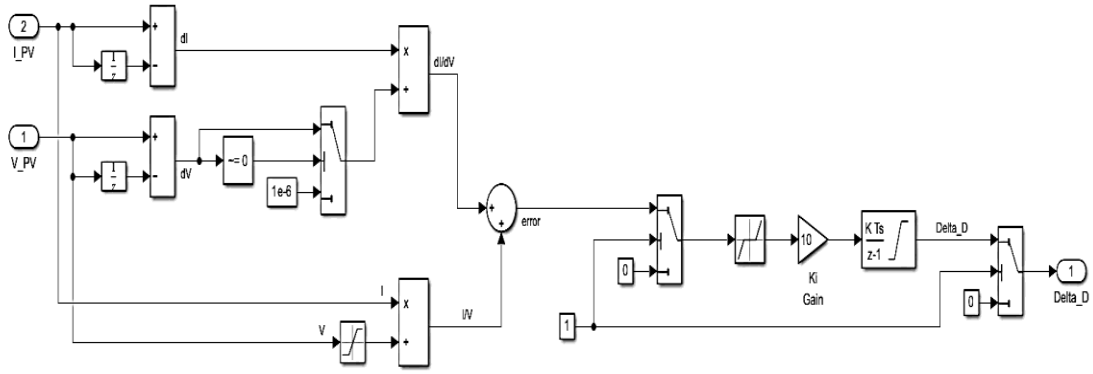

Figure 4. 4 Incremental Conductance Simulation

Figure 4.4 shows a Maximum Power Point Tracking (MPPT) control strategy for a photovoltaic system, utilizing the Incremental Conductance (INC) algorithm. The input signals, I_{PV} (PV current) and V_{PV} (PV voltage) are processed to compute the incremental changes in current (dI) and voltage (dV). The incremental conductance (dI/dV) and the instantaneous conductance (I/V) are compared to determine the error signal, which indicates the deviation from the maximum power point (MPP).

A decision-making process uses this error signal to adjust the duty cycle (D) of the system's power converter. This is achieved through a control loop that includes an integrator with a gain (Ki) to ensure stability and convergence. A discrete-time implementation is evident from the inclusion of a delay block (z^{-1}), which facilitates real-time processing.

The control output ΔD, represents the incremental adjustment in the duty cycle required to track the MPP. This adjustment minimizes the error signal and ensures that the PV system operates at its optimal power output.

4.1.1.2 State of Charge (SOC) control

In Figure 4.3, the State of Charge (SOC) control mechanism is designed to manage the energy storage system (ESS) efficiently and safely. The SOC is continuously monitored and compared to a predefined threshold of 90%, which is the maximum allowable charge limit. This prevents overcharging, protecting the ESS from performance degradation and potential risks. The SOC value is processed through a comparator block. If the SOC is below the threshold, the system permits Pulse-Width Modulation (PWM) signals, generated by the MPPT and voltage regulation, to enable energy flow between the PV array, ESS, and load. If the SOC exceeds 90%, the comparator activates a switch block to stop PWM signal generation, halting further charging of the ESS. This automated logic ensures the ESS operates within safe limits while maintaining efficient energy harvesting.

The switch block dynamically controls PWM signals in real time, optimizing energy utilization and prioritizing ESS longevity and safety. This SOC control mechanism contributes to the overall stability, reliability, and sustainability of the DC microgrid, adapting effectively to varying conditions of energy demands and generation.

4.1.1.3 Discrete Proportional-Integral (PI) Controller

The Simulink model includes a voltage regulation mechanism in Figure 4.3, to stabilize the DC bus Voltage (Vdc), which is essential for maintaining the reliability and performance of the DC microgrid. The system continuously monitors (V_{dc}) and compares it to a reference voltage, generating an error signal processed by a discrete Proportional-Integral (PI) controller. The PI controller uses proportional (K_p) and integral (K_i) actions to minimize voltage deviations, addressing immediate and cumulative errors to ensure accurate and stable voltage regulation.

The control signal (ramp_out) generated through the PI controller is smoothed using a ramp generator, preventing abrupt changes that could destabilize the system. This ensures gradual voltage adjustments, maintaining the stability of the microgrid. The mechanism is designed to handle variations such as load changes and transient conditions, keeping Vdc within the desired range for stable operation of connected loads and energy storage systems. This regulation strategy enhances the efficiency and reliability of a system, supporting the integration of intermittent renewable energy sources like photovoltaic arrays. By ensuring precise and adaptive voltage control, the mechanism contributes to the stability and sustainability of the DC microgrid.

Therefore, MPPT, SOC control, and voltage regulation ensure the PV system operates efficiently while maintaining system safety and stability. The MPPT maximizes power extraction from the PV array, the SOC control safeguards the energy storage system from overcharging, and the voltage regulation ensures consistent and reliable power delivery to the DC microgrid.

4.2 Simulation for developed Battery model

Simulation of the Nickel-Metal Hydride (Ni-MH) battery model, a vital component of the energy storage system within the DC microgrid. The Ni-MH battery is known for its ability to provide high energy density, long cycle life, and efficient energy storage, making it an ideal choice for renewable energy systems. The model developed in this work simulates critical battery behaviour, including state-of-charge (SOC) management, charging and discharging dynamics, and efficiency under varying operational conditions. This simulation is essential for understanding the battery's performance, optimizing its integration into the microgrid, and ensuring stable and reliable energy storage.

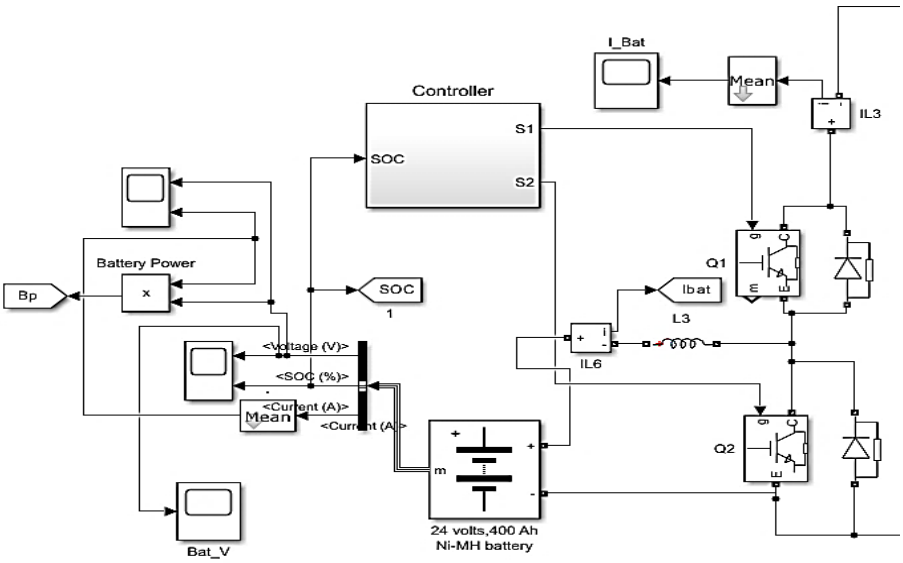

Figure 4. 5 Simulation of Battery Model (Ni-MH,24V,400 Ah)

Figure 4.5 illustrates a battery management and control system for a 24V, 400Ah Nickel-Metal Hydride (Ni-MH) battery, focusing on monitoring, control, and regulation. The system calculates battery power by multiplying the measured voltage and current, with both parameters continuously monitored. The State of Charge (SOC) estimation block uses the battery current and voltage to determine the remaining capacity, which is then fed into the controller for decision-making.

The controller generates two control signals, S1 and S2, to regulate the operation of the power electronic switches (Q1 and Q2), enabling controlled charging and discharging of the battery. A bidirectional inductor (L3) facilitates energy transfer during these operations. The current flowing through the battery (I_{Bat}) and the inductor (I_{L6}) is measured and processed through mean blocks to smoothen fluctuations, ensuring stable operation. The output current (I_{L3}) represents the energy supplied to the external load.

This setup ensures that the battery operates within safe voltage and current limits, protecting it from overcharging or deep discharge. Overall, the system demonstrates an efficient and robust approach to managing energy flow in battery-powered applications. Table 4.2 shows the parameters of the battery management system. These parameters are critical for ensuring safe and efficient system operation under various conditions.

Table 4. 2 Parameters for the Battery model

Parameters	Range
Nominal Voltage(V)	120V
Rated Capacity (Ah)	250Ah
Maximum Capacity (Ah)	277Ah
Fully Charged Voltage(V)	128.34V
Nominal discharge current(A)	21A
Initial SOC	90%

4.2.1 Control Strategies in Battery Energy Storage System

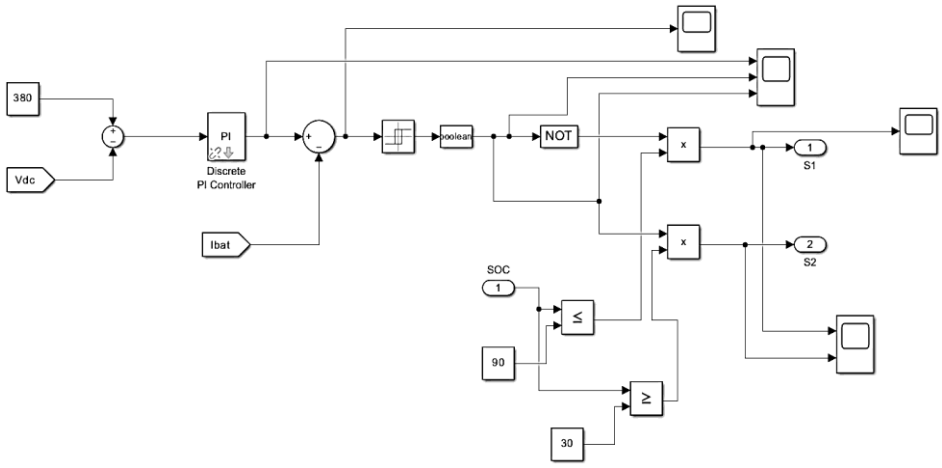

Figure 4. 6 Control Strategies for Battery

Figure 4.6 represents a Simulink block diagram of a control system designed to manage a battery in a DC microgrid. A discrete Proportional-Integral (PI) controller regulates the charging and discharging current (Ibat) by minimizing the error between a reference voltage of 380 V and the measured DC voltage (Vdc). The system monitors both storage devices' state of charge (SOC) and uses logical conditions to ensure safe and efficient operation.

For the battery, charging is disabled when the SOC exceeds 90%, and discharging stops when the SOC drops below 30%, protecting it from overcharging and deep discharge. Boolean logic, including comparators and a NOT gate, generates control signals for switches (S1 and S2) that determine the operational mode of each storage device.This integration of SOC-based logic with the PI control loop ensures stable voltage regulation and optimal energy management.

4.3 Simulation for developed Supercapacitor model

This section presents the simulation of the developed Electric Double-Layer Capacitor (EDLC) supercapacitor model, which is an integral component of the energy storage system within the DC microgrid. EDLCs, also known as supercapacitors, are characterized by their ability to deliver high power output and rapid charge/discharge cycles, making them suitable for stabilizing voltage and providing short-term energy support.

The model simulates key parameters of EDLCs, including energy density, charge/discharge efficiency, and performance under various load conditions. This simulation aims to assess the role of EDLCs in improving the DC microgrid's overall performance, particularly in terms of power management and response to sudden fluctuations.

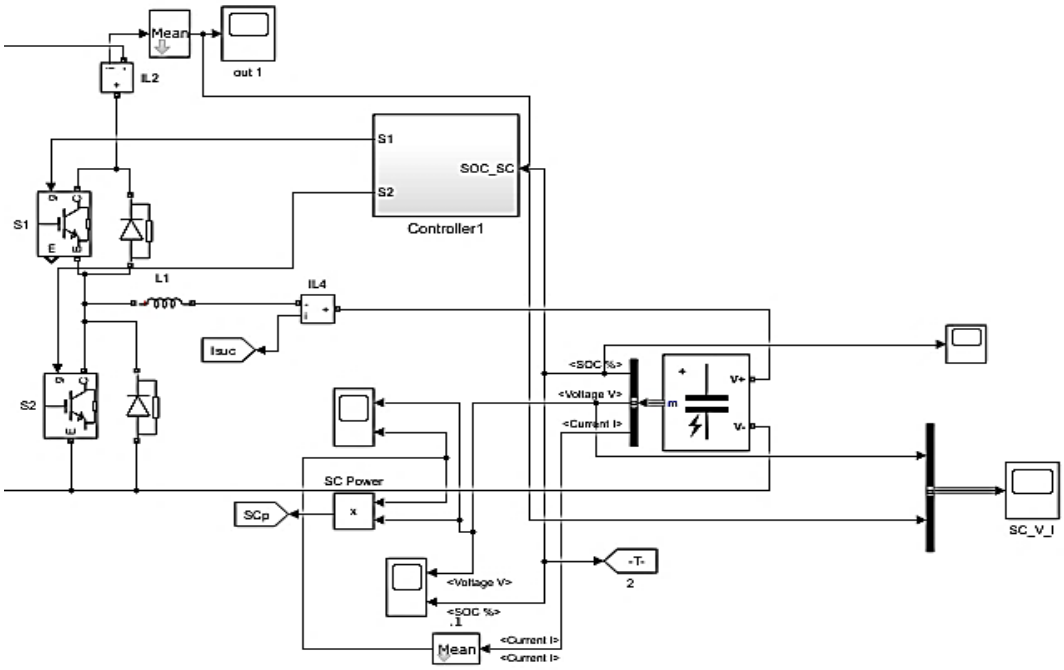

Figure 4. 7 Simulation of the developed Supercapacitor Model

Figure 4.7 illustrates the Simulink model of a supercapacitor-based energy storage system integrated into a DC microgrid. The design incorporates a detailed structure of power electronic switches, controllers, and monitoring components for dynamic operation and control. The system employs a bi-directional DC-DC converter connected to the supercapacitor, managed by a control block labeled "Controller1." This controller regulates the state of charge (SOC) of the supercapacitor through switching signals (S1 and S2). The SOC is monitored using the "SOC_SC" subsystem, which processes voltage and current signals to maintain the supercapacitor's operational limits.

Power flow is monitored using a power computation block ("SC Power"), which calculates the instantaneous power of the supercapacitor based on voltage and current inputs. The output is used for performance evaluation. Additionally, a measurement block computes the mean value of key parameters such as voltage, current, and SOC, ensuring smooth operation.

Inductors (L1, L2) and a resistor form part of the converter's electrical circuit to manage current and voltage dynamics. The "I_SUC" component measures the current flowing to and from the supercapacitor. Outputs from the system, including voltage, current, and SOC, are displayed through the respective signal monitors.

This configuration highlights the interplay between control strategies and power electronics in maintaining system stability, efficient energy utilization, and the supercapacitor's longevity within a DC microgrid. Table 4.3 shows the parameters of the supercapacitor model.

Table 4. 3 Parameters for the Supercapacitor Model

Parameters	Range
Rated Capacitance(F)	3300F
DC equivalent Series resistance(ohms)	0.04 ohm
Rated Voltage(V)	3.8 V
Molecular radius(m)	1e-12
Operating temp.	$70^{o}C$

4.3.1 Control Strategies in Supercapacitor Energy Storage System

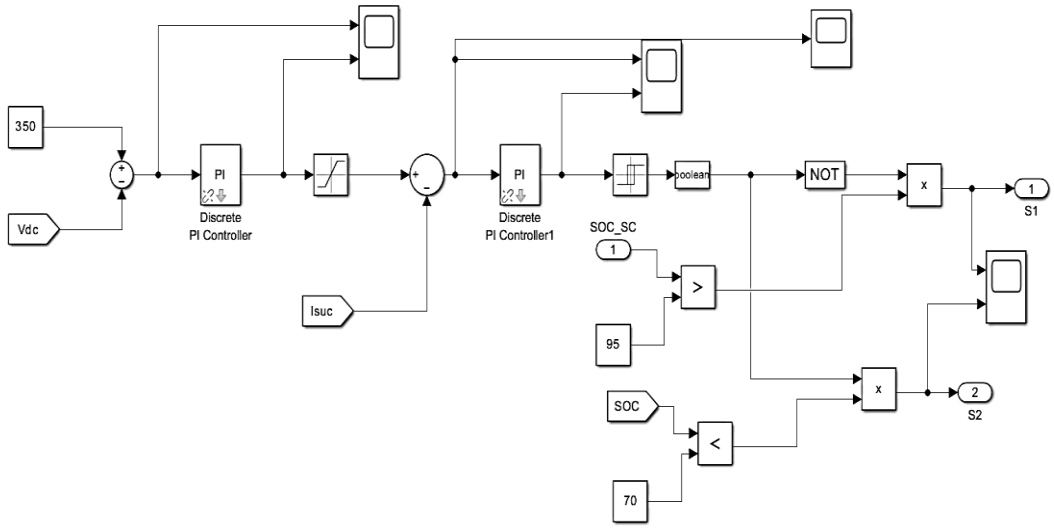

Figure 4. 8 Control strategies for Supercapacitor

Figure 4.8 represents a Simulink block diagram of a control system designed to manage a supercapacitor in a DC microgrid. A discrete Proportional-Integral (PI) controller regulates the charging and discharging current (Isuc) by minimizing the error between a reference voltage of 380 V and the measured DC voltage (Vdc). The system monitors both storage devices' state of charge (SOC) and uses logical conditions to ensure safe and efficient operation.

For supercapacitors, similar SOC-based logic is applied, but with different thresholds: charging stops at 95%, and discharging halts below 70%. Boolean logic, including comparators and a NOT gate, generates control signals for switches (S1 and S2) that determine the operational mode of each storage device.

This integration of SOC-based logic with the PI control loop ensures stable voltage regulation and optimal energy management. By maintaining safe operating limits for supercapacitors, the system enhances reliability and efficiency, while supporting the dynamic demands of the DC microgrid.

4.4 Simulation for developed Fuel cell model

Simulation of the developed fuel cell model, which is a key component for providing backup power and enhancing the reliability of the DC microgrid. Fuel cells, specifically proton exchange membrane (PEM) fuel cells, are widely recognized for their high efficiency, low emissions, and ability to generate continuous power.

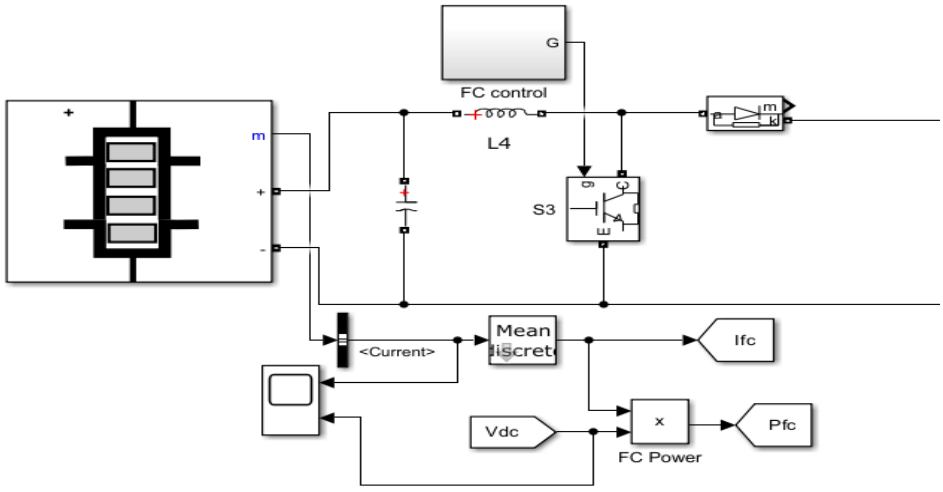

Figure 4. 9 Simulation for Fuel Cell Model

The model simulates the dynamic behavior of the fuel cell, including its voltage and current characteristics, efficiency, and response to varying load demands. By simulating the fuel cell's performance under different operational conditions, this section aims to evaluate its integration within the microgrid and its contribution to the system's overall stability and energy management.

Figure 4.9 illustrates the Simulink model of a fuel cell integrated into a DC microgrid, functioning as a standby energy source. The fuel cell is connected to the DC microgrid through

a unidirectional DC-DC converter, regulated by a control block labeled "FC Control." This controller ensures the efficient operation of the fuel cell by managing the switching signal (S3) and maintaining the desired output voltage and current levels. The inductor (L4) and capacitor are integrated into the circuit to smoothen the current flow and stabilize the voltage, respectively.

The model includes a power computation block ("FC Power") that calculates the instantaneous power output of the fuel cell based on its voltage (Vdc) and current (Ifc). This information is used to monitor the performance and contribution of the fuel cell during operation. A mean block processes the current signal to ensure consistent power delivery.

Table 4. 4 Parameters of the Fuel Cell

Parameters	**Range**
Nominal Operating voltage	45V
Nominal Operating current	133.3 A
Internal resistance	0.07833 ohms
Maximum operating voltage	37V
Maximum operating current	225A
No. of cells	65
Nominal composition (%) $[H_2, O_2, H_2O(Air)]$	[99.95, 21,1]
Temperature (℃)	65

The configuration also incorporates measurement blocks to monitor critical parameters, such as current (Ifc) and voltage (Vdc), providing real-time feedback for system analysis. The fuel cell is a reliable and sustainable energy source, ensuring continuous power supply and enhancing the resilience of the DC microgrid in standby mode. The above Table 4.4 shows the parameters of the ELDC Fuel cell.

4.4.1 Control Strategies in Fuel Cell

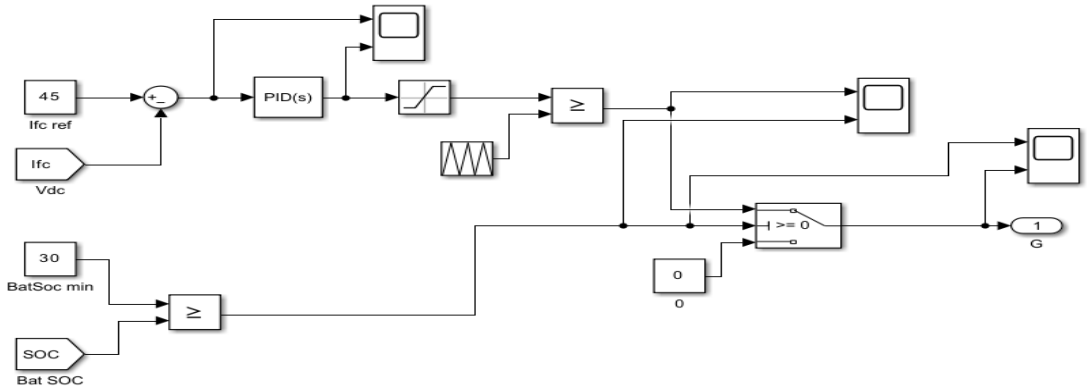

Figure 4. 10 Control strategies for Fuel cell

Figure 4.10 illustrates the control strategy design for managing a fuel cell system integrated with a hybrid storage device. The primary objective of this control system is to regulate the fuel cell current, protect the battery from deep discharge, and ensure stable operation of the DC bus. At the system's core, a reference fuel cell current (I_{fc_ref}) is set to 45A, which serves as the target current. The actual fuel cell current (I_{fc}) is subtracted from the reference to generate an error signal. This error is processed by a PID controller, which adjusts its output to regulate the fuel cell's performance. A limiter is incorporated to constrain the PID output, ensuring control action remains within safe bounds.

Additionally, the system monitors the battery's state of charge (SOC) and compares it against a predefined minimum threshold of 30%. This comparison ensures the battery does not discharge below the critical level, thereby protecting its longevity. If the SOC falls below the threshold, the control logic disables certain operations by switching off the gating signal. The DC bus voltage (Vdc) is monitored to maintain system stability and ensure consistent energy delivery.

4.5 Load demands for the DC Microgrid

This section details the simulation of DC load demands in the 40 kW DC microgrid, a critical aspect in evaluating the system's behavior under different load conditions. The simulation models the integration of multiple DC loads connected to the DC bus, incorporating protective elements such as circuit breakers for operational flexibility and reliability. Additionally, the role of capacitors in stabilizing voltage during transient fluctuations is simulated to assess their impact on overall system performance. By simulating these components, this analysis provides

valuable insights into the efficient distribution of power, voltage regulation, and the stability of the microgrid under dynamic load conditions.

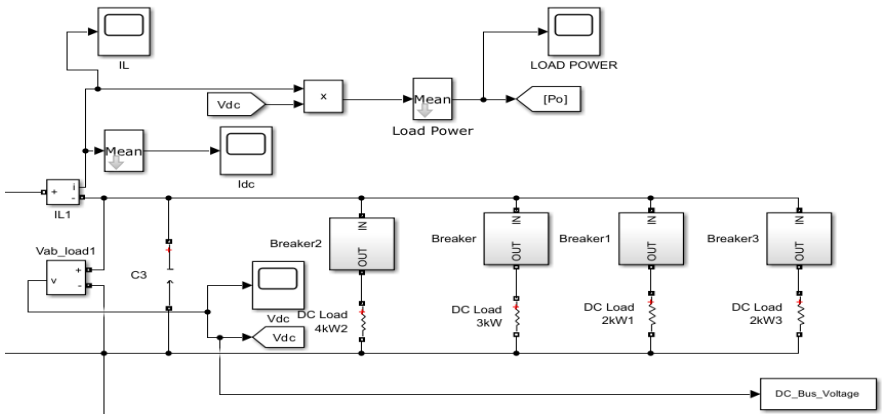

Figure 4. 11 Load analysis

Figure 4.11 illustrates the load analysis of a 40 kW DC microgrid operating at a nominal voltage of 380 V DC. The configuration models multiple DC loads connected to the DC bus and evaluates the system's performance under varying load conditions. The loads are distributed into three separate branches, each with individual circuit breakers for protection and control. These loads are specified as follows: a 4-kW load, a 3-kW load, and two 2-kW loads summing up to a total load of 11 kW in this scenario. The circuit breakers ensure that specific loads can be isolated or connected as required, enhancing system reliability and operational flexibility.

Voltage and current measurements are taken across the loads using sensors such as Vdc and I_{dc}. These measurements are fed into a power computation block to determine the real-time power consumed by the loads. The load power is averaged using a mean block to smooth fluctuations and provide stable output for monitoring and analysis.

A capacitor (C3) connected to the DC bus helps stabilize the voltage by compensating for transient variations in load demand. The DC bus voltage is monitored to ensure it remains close to the nominal 380 V, maintaining the stability and efficiency of the microgrid. This setup enables efficient load analysis, real-time monitoring, and control of power distribution within the DC microgrid, making it a robust system for handling variable load demands while ensuring stable voltage at the DC bus.

4.6 Simulation Results: Case Studies for Developed DC Microgrid

This section presents a series of case studies exploring power management strategies in DC microgrids under different configurations. Each case highlights specific scenarios to examine the dynamic behavior of power flows and the interaction between system components. The overarching objective is to identify strategies that ensure reliable and efficient operation while addressing real-time power balance challenges.

4.6.1 Case:1 Power management in DC Microgrid without Battery ($P_{pv} = P_{load}; P_{Bat}; P_{sc}$)

In this case, investigates the PV power (P_{pv}) directly matched to the load power (P_{load}). The absence of energy storage presents a unique challenge, as power balance must be maintained instantaneously. The study focuses on the dynamic response of the microgrid to variations in solar generation and load demand.

Integrating renewable energy sources, such as photovoltaic (PV) systems, into DC microgrids has emerged as a promising solution to enhance energy sustainability and reduce dependency on traditional power grids. One of the core challenges in managing such systems is balancing load power (the power demand of the system) with PV power (the power generated by the photovoltaic panels), as both these factors fluctuate over time due to changing environmental conditions, load variations, and solar availability. In this case, the dynamic behaviour of load power and PV power over 5 seconds are analyzed to explore how the DC microgrid responds to changes in both demand and generation.

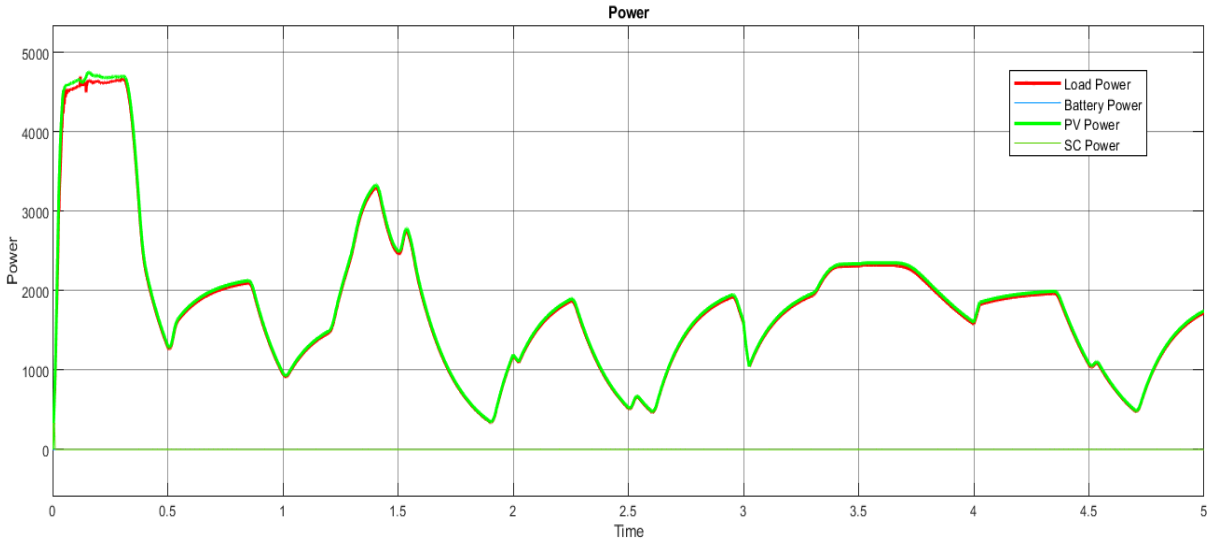

Figure 4. 12 Power Management for Case 1

Figures 4.12 and 4.13 show the Power output and Dynamic response analysis in the DC link bus respectively. At the initial overshoot period at t=0.3 sec, the DC link voltage experiences a rapid rise, peaking at approximately 430 V due to the charging of the DC link capacitor. This initial overshoot, a characteristic of system initialization, is carefully regulated to remain within design limits. Simultaneously, the load power reaches 1291 W, while the PV power is 1312 W at t = 0.5 seconds, indicating a slight surplus of power generation to meet the initial demand. As the voltage stabilizes, a damping phase occurs between t = 0.3 and 1.0 seconds, where the DC link voltage decreases to 414 V at t = 0.5 seconds and further stabilizes at 420 V at t = 1.0 seconds. This stabilization is achieved through the use of proportional-integral (PI) controllers, which ensure a smooth transition to steady-state conditions. During this phase, load power decreases to 951.5 W, while PV power adjusts to 967.6 W, maintaining equilibrium between supply and demand. In a transient period between t = 1.0 and 3.5 seconds, with fluctuations in voltage due to dynamic changes in load power. At t = 1.5 seconds, the load power surges to 2469 W, and PV power increases to 2502 W, causing the DC link voltage to drop to 390.5 V. Similarly, at t = 3.0 seconds, load power decreases to 1593 W, while PV power stabilizes at 1618 W, yet the voltage dips to 402.7 V due to transient effects. The most severe drop occurs at t = 3.5 seconds, where load power peaks at 2314 W, and PV power reaches 2340 W, resulting in the lowest voltage point of 344.7 V. These fluctuations underscore the challenges in maintaining voltage stability during periods of varying load demand.

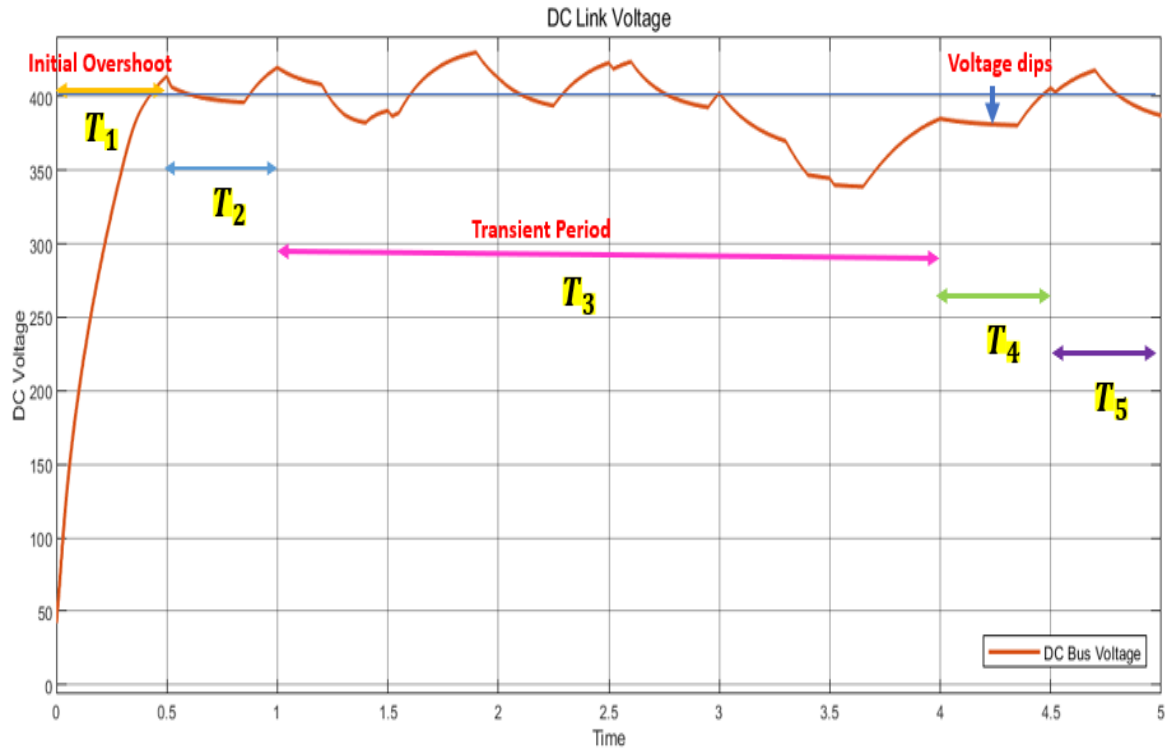

Figure 4. 13 Dynamic Response Analysis of DC Link Voltage for Case 1

The system demonstrates its recovery capabilities between t = 3.5 and 4.5 seconds, as the voltage begins to rise from its lowest point. At t = 4.0 seconds, the voltage recovers to 385.2 V, with load power at 1580 W and PV power at 1604 W, reflecting the system's ability to restore balance. At t = 4.5 seconds, the voltage further improves to 406 V, while load power and PV power align at 1067 W and 1085 W, respectively. Between t = 4.5 and 5.0 seconds, the DC microgrid achieves steady-state operation, with the DC link voltage stabilizing at around 387.3 V. During this time, load power rises to 1724 W, while PV power generation adjusts to 1747W, maintaining stable and dependable system performance. Table 4.5 represents the data for power management without a battery model.

Table 4. 5 Parameters for Power Management without Battery

Time	Load Power (W)	PV Power (W)	DC link voltage(V)
0.5	1291	1312	414
1	951.5	967.6	420
1.5	2469	2502	390.5
2	1181	1196	412.8
2.5	519.6	529.5	**423.1**
3	1593	1618	402.7
3.5	2314	2340	**344.7**
4	1580	1604	385.2
4.5	1067	1085	406
5	1724	1747	387.3

Figure 4.14 (a) shows the State of charge of the battery and Figure 4.14 (b) shows the State of charge of the Supercapacitor for case 1. SOC of a battery or supercapacitor gradually increases and then becomes constant, it suggests that the system is in a state where no significant charging or discharging is occurring. The battery or SC may have reached a stable charge level, with no active energy exchange.

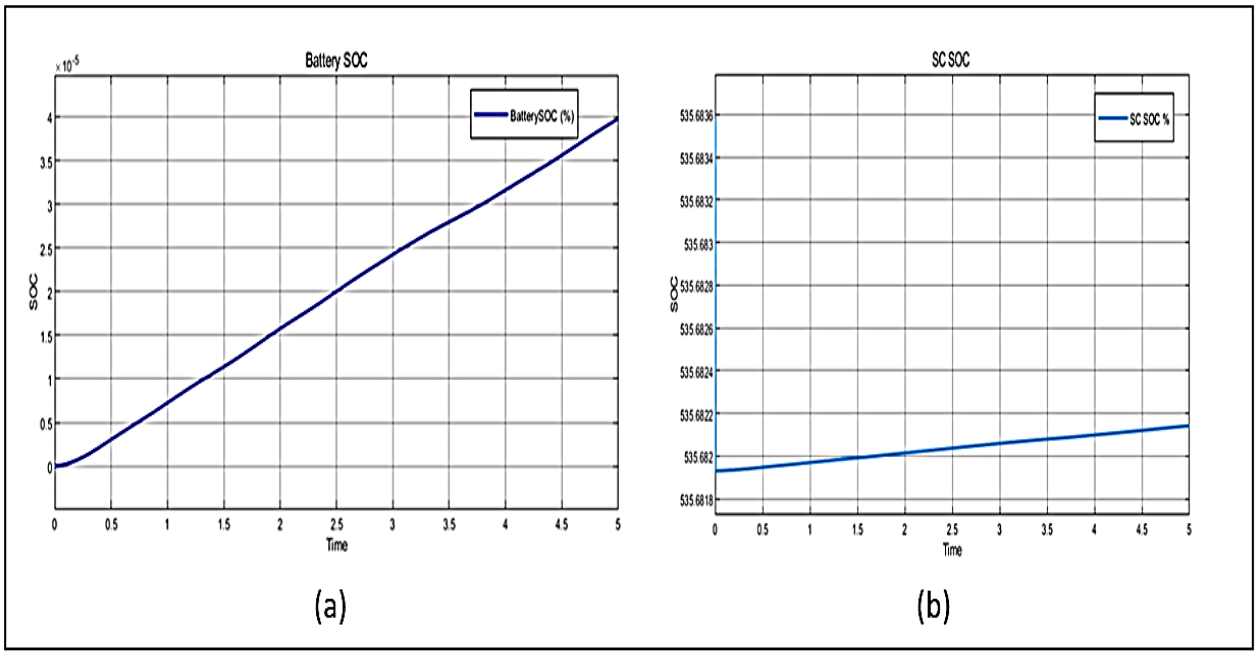

Figure 4. 14 (a) Battery SOC (b) SC SOC

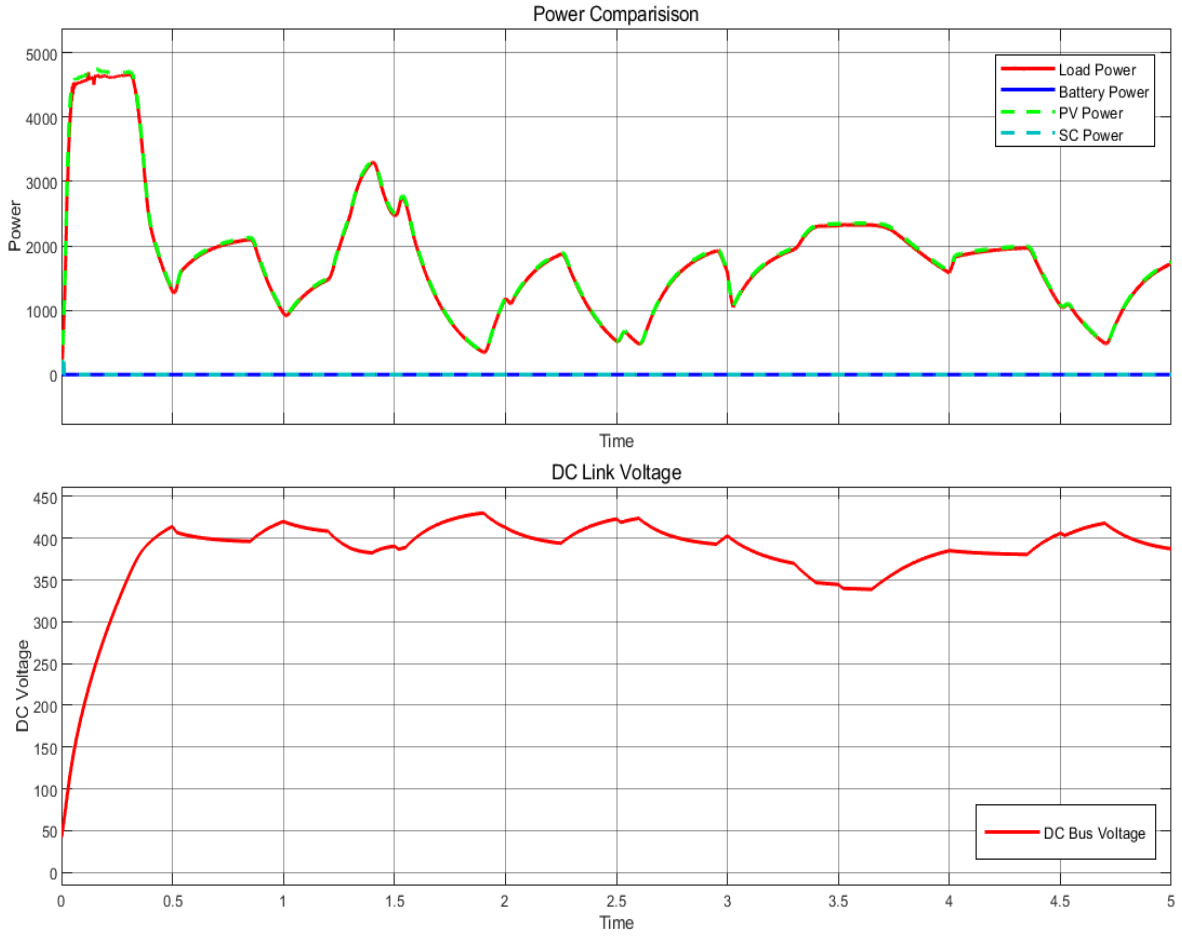

Figure 4. 15 Power Output and DC Link Voltage Profile for Case 1

Figure 4.15 represents the analysis of the dynamic response in a DC microgrid. Therefore, Calculate the system's dynamic response concerning key performance metrics, such as peak overshoot, peak undershoot, settling time, steady-state voltage, and voltage deviation. Table 4.6 represents the parameters of the dynamic response for case 1.

Peak Overshoot: The peak overshoot occurs when the system's voltage exceeds the steady-state value. In this case, the voltage at 2.5 seconds reaches a maximum of 423.1 V. The steady-state voltage is 387.3 V. Therefore, the peak overshoot is calculated as:

$$V_{overshoot} = maxV_{dc}(t), for t > t_0 \quad (5.1)$$

$$V_{overshoot} = 423.1V(2.5sec)$$

$$\text{Peak Overshoot} = V_{max} - S_{teady\text{-}state} \quad (5.2)$$

Peak overshoot = 422.2 – 380 = 43.8V

Peak Undershoot:

$$V_{undershoot} = min\{V_{dc}(t)\}, for\ t > t_0 \quad (5.3)$$

Peak undershoot occurs at a time of 3.5 sec with a voltage of 344.7 V.

Peak undershoot = 387.3 -344.7 = 42.6 V

Settling time:

$$t_{settling} = t_s - t_0 \quad (5.4)$$

From Figure 5.9, voltage fluctuates around 0.1 to 0.5 sec, to stabilize near the steady state value. Assume, settling time = 0.5 sec

Steady-state Voltage:

Steady-state Voltage = 387.3 V (5 sec)

Maximum Peak overshoot

$$\text{Maximum Peak overshoot (\%)} = \frac{Peak\ overshoot}{steady\ state\ voltage} \times 100 \quad (5.5)$$

$$\text{Maximum Peak overshoot (\%)} = \frac{35.8\,V}{387.3\,V} \times 100 = 9.24\%$$

Voltage deviation:

Voltage deviation = Excepted steady state voltage – Actual steady state voltage (5.6)

Voltage deviation = 400 V – 387.3 V = 12.7 V

Table 4. 6 Dynamic Response Analysis for Case 1

Parameters	Range
Peak overshoot voltage	43.8 V (2.5 sec)
Peak undershoot voltage	42.6V (3.5 sec)
Steady-state voltage	387.3V (5 sec)
Settling time	0.5 sec
(% M_P) Maximum Peak overshoot	9.24%
(ΔV) $Voltage\ deviation$	12.7V

In this case, the system performance analysis, reveals several key insights regarding its stability and efficiency. The system exhibits moderate overshoot, which could affect sensitive components and overall performance. One of the primary concerns is the lack of activity from the energy storage device, particularly under increasing and decreasing load conditions, which could challenge the system's ability to maintain voltage stability. The absence of storage support leads to an inability to efficiently buffer voltage fluctuations, which may cause potential damage to components and reduce system efficiency. While the system does maintain relative stability without the energy storage, this is not sustainable under more demanding scenarios such as rapid load changes or reduced PV availability. Therefore, integrating a battery system would enhance the robustness of the PV system, ensuring more reliable operation and safeguarding sensitive components under variable conditions.

4.6.2 Case:2 Power management in DC Microgrid with Battery

$(P_{pv} = minimum, P_{Bat\_} < P_{load})$

When the photovoltaic power output (P_{pv}) is at its minimum, and the load demand (P_{load}) exceeds the photovoltaic output, the battery ($P_{Bat\_}$)becomes useful by discharging to compensate for the power deficit.

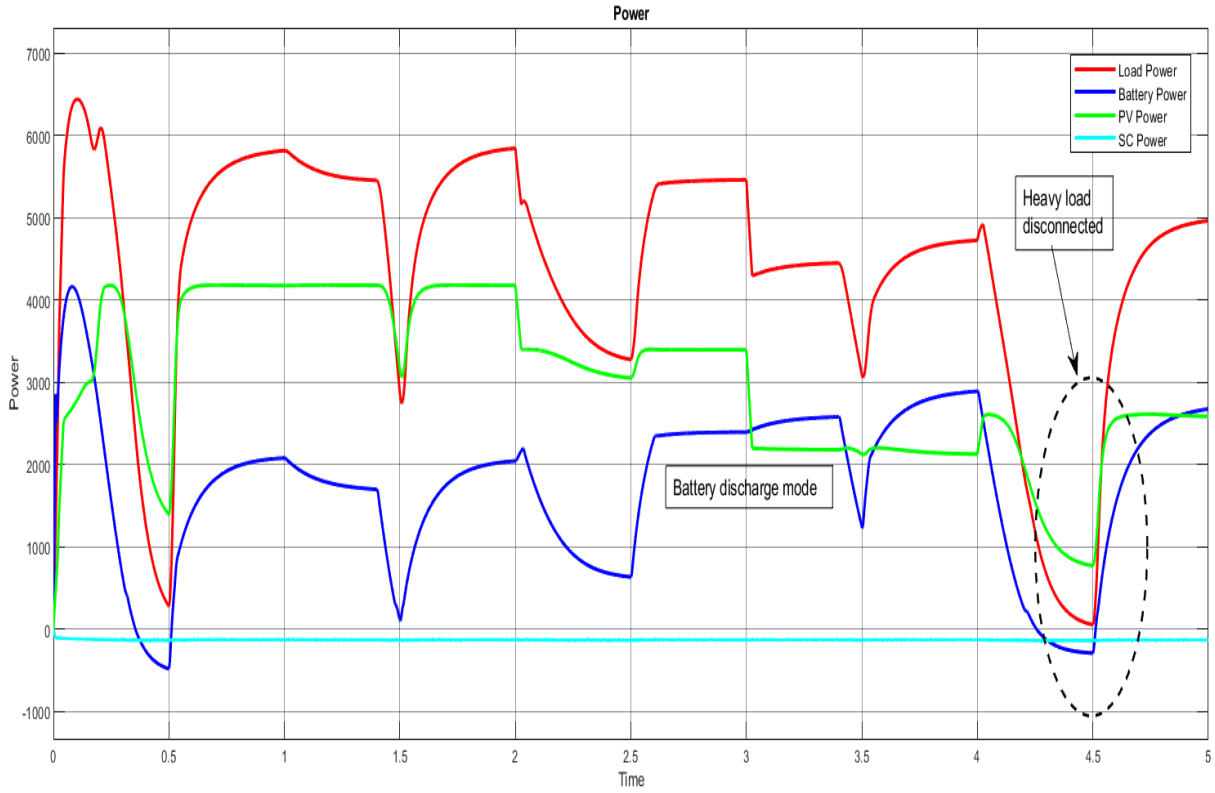

Figure 4. 16 Power Management for Case 2

During the daytime in spring or monsoon seasons, rapidly changing weather, such as passing clouds or intermittent sunlight, causes fluctuations in PV generation. Simultaneously, varying load demands, typical in industrial or commercial settings, create dynamic conditions that the battery compensates for effectively.

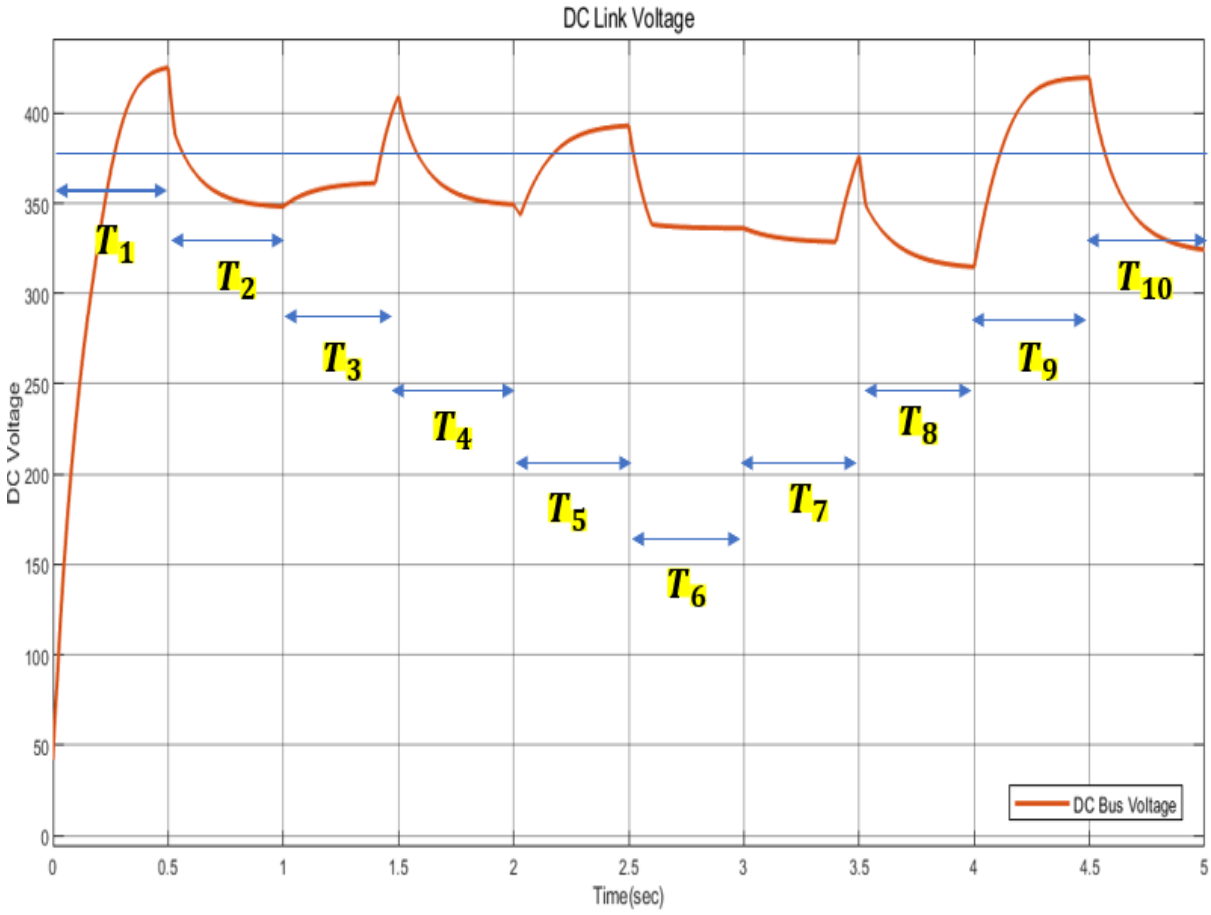

Figure 4. 17 Dynamic Response Analysis of DC Link Voltage for Case 2

Figures 4.16 and 4.17 illustrate the performance of a DC microgrid system utilizing only a battery as its energy storage component to manage dynamic load and generation conditions. Hence, the load demand exceeds the PV generation, the battery discharges to compensate for the deficit. Conversely, during periods of excess PV generation, the battery absorbs the surplus energy, ensuring system stability and preventing overvoltage. The voltage remains near the nominal value of 380V under most conditions, despite fluctuations caused by load changes. However, during certain periods, such as at 0.5 seconds, 2.5 seconds, and 4.5 seconds, the DC link voltage experiences dip due to sudden increases in load demand. These transient dips are mitigated through the battery's swift response, ensuring rapid recovery and maintaining operational stability. Table 4.7 represents the parameters for power management with battery for case 2.

Table 4. 7 Parameters for Power Management with Battery Case 2

Time	Load Power (W)	PV Power (W)	Battery Power (W)	DC link voltage(V)
0.5	279.9	1396	-480.1	425
1	5817	4177	2081	348.2
1.5	2863	3156	110	409.3
2	5845	4179	2045	349.4
2.5	3277	3054	636.4	392.9
3	5460	3395	2696	336.2
3.5	3091	2129	1242	376.4
4	4725	2128	2892	314.8
4.5	56.13	772.3	-288.6	419.6
5	4965	2587	2677	324.3

At 1.5 seconds, the load decreases to 2863W, and PV power nearly meets the demand, requiring only 110W from the battery and stabilizing the voltage at 409.3V. As the load increases again to 5845W at 2 seconds, the battery discharges 2045W, and the voltage dips to 349.4V. At 2.5 seconds, with a load of 3277W and PV power at 3054W, the battery supplements 636.4W, stabilizing the voltage at 392.9V. At 3 seconds, the load rises to 5460W, and the battery discharges 2696W to meet the deficit, causing a significant voltage drop to 336.2V. At 3.5 seconds, the load reduces to 3091W, and with PV power at 2129W, the battery supplies 1242W, maintaining the voltage at 376.4V.

At 4 seconds, the load increases to 4725W while PV power remains low at 2128W, requiring the battery to discharge 2892W, resulting in the lowest voltage of 314.8V. By 4.5 seconds, the load drops significantly to 56.13W, and PV power at 772.3W allows the battery to charge (-288.6W), increasing the voltage to 419.6V. Finally, at 5 seconds, the load rises to 4965W, and the battery discharges 2677W alongside PV power of 2587W, stabilizing the voltage at 324.3V. The battery effectively balances the energy supply and demand, mitigating voltage fluctuations and ensuring continuous operation despite load and generation variations. It plays a crucial role in stabilizing the system during both high-demand and surplus conditions, where it

compensates for energy imbalances. However, the supercapacitor could further optimize the system's performance, particularly in transient compensation and rapid response scenarios.

During sudden load surges or PV generation dips, the supercapacitor could rapidly supply or absorb power, handling the short-term, high-power needs that may cause significant voltage drops. For instance, when the load spikes at 1 second, the supercapacitor could quickly supply energy to prevent the voltage from dropping significantly, thereby minimizing stress on the battery and enhancing the system's voltage stability. This would allow the battery to focus on long-term energy balancing rather than reacting to fast transients. When PV generation exceeds the load, as seen at 0.5 seconds or 4.5 seconds, the supercapacitor could store surplus energy efficiently for future use, reducing the need for deep battery discharges and prolonging the battery's lifespan.

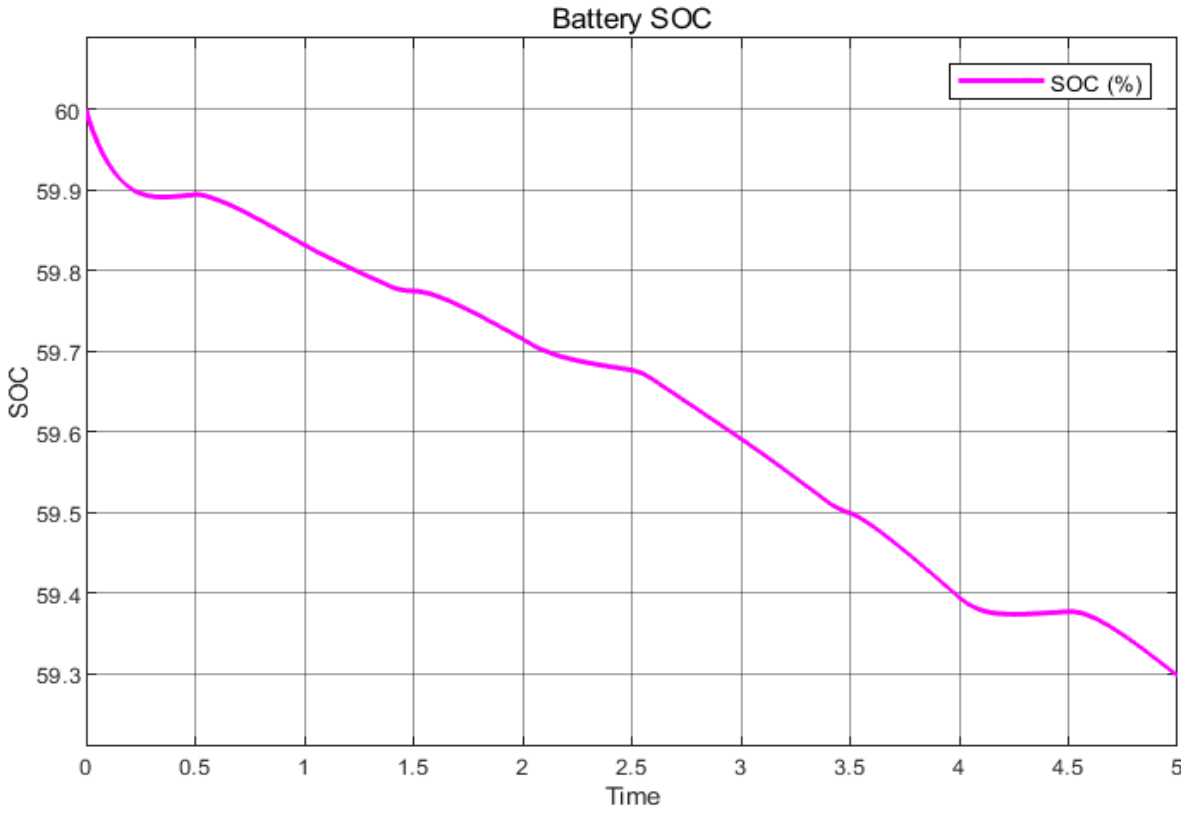

Figure 4. 18 Battery SOC for case 2

By incorporating a supercapacitor, the system would gain faster response times, improved voltage regulation, and increased system efficiency, while the battery continues to handle medium- to long-term energy balancing. Together, these two storage systems would work in

synergy, ensuring a more robust and reliable DC microgrid, capable of maintaining both steady-state and transient conditions.

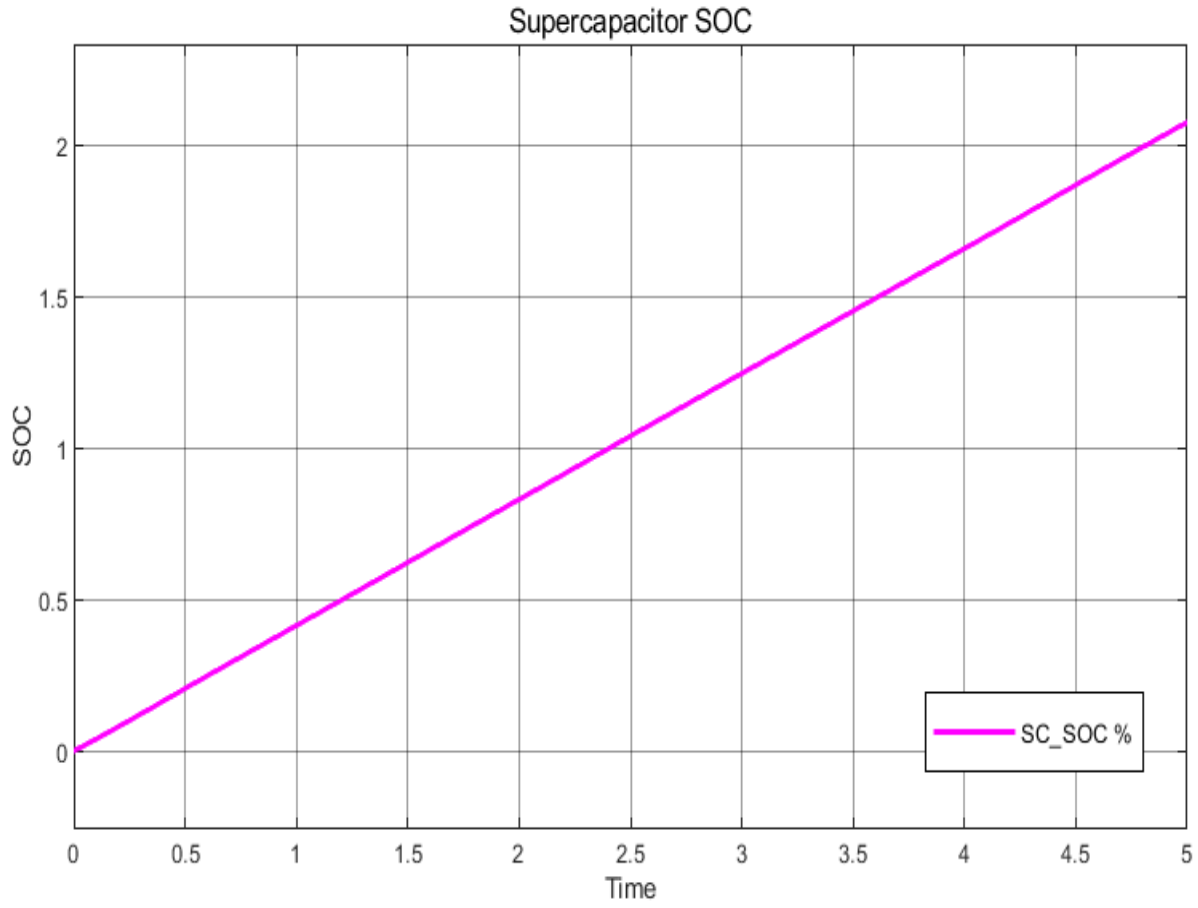

Figure 4. 19 Battery SOC for case 2

Figure 4.18 shows the battery's State of charge, and Figure 4.19 shows the supercapacitor's State of charge for case 2. When the supercapacitor's SOC gradually rises and then stabilizes while the battery remains the sole active energy storage, it suggests that the system has reached a steady state. In this condition, the battery is efficiently managing the energy balance.

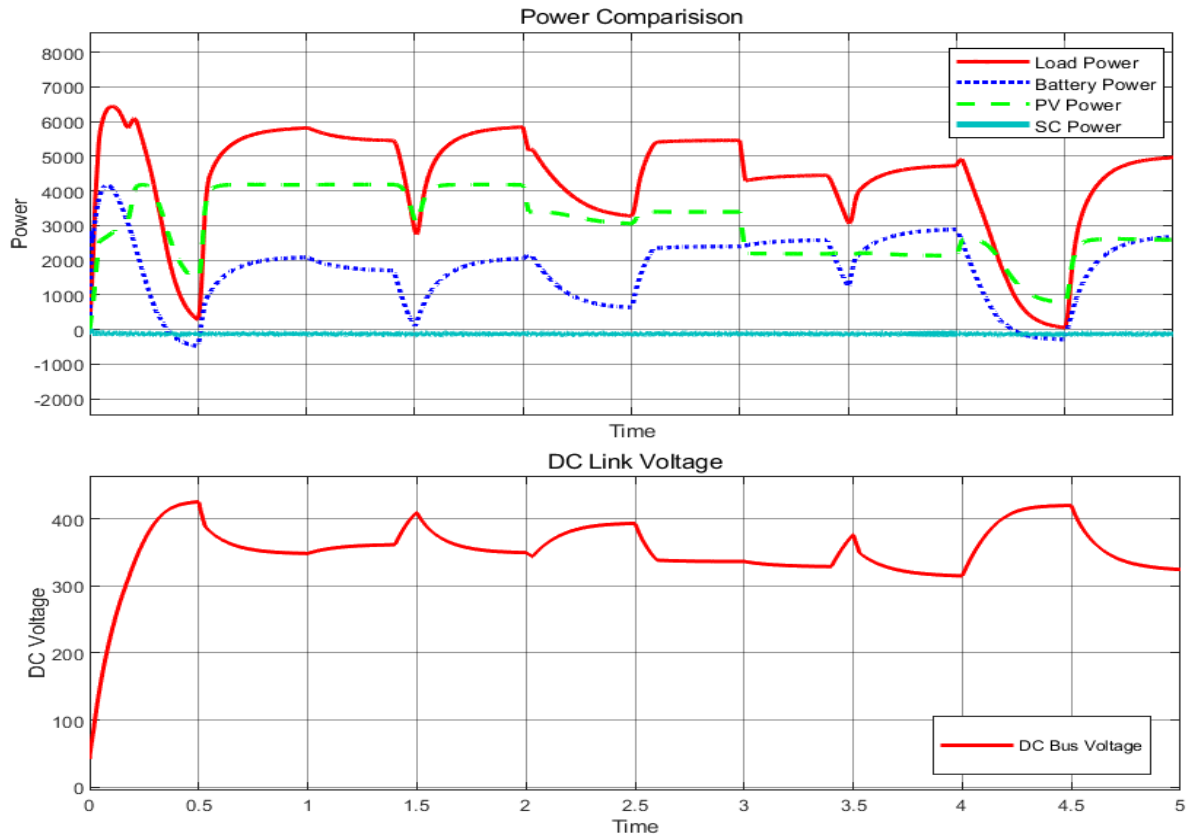

Figure 4. 20 Power Output and DC Link Voltage Profile for Case 2

Figure 4.20 represents the analysis of the dynamic response in a DC microgrid. Therefore, Calculate the system's dynamic response concerning key performance metrics, such as peak overshoot, peak undershoot, settling time, steady-state voltage, and voltage deviation. Table 4.8 represents the Dynamic response parameters for case 3.

Peak Overshoot:

$$V_{overshoot} = maxV_{dc}(t), for t > t_0$$

$V_{overshoot} = 425.02\ V(0.5sec)$

Stead state voltage = $\frac{425+348+310+350+392+335+376+320+419+335}{10} = \frac{3610}{10} = 361\ V$

Peak overshoot = 425.02-380 = 45V

Peak Undershoot:

$$V_{undershoot} = min\{V_{dc}(t)\}, for\ t > t_0$$

Peak undershoot occurs at time 4 sec with a voltage of 319.86 V.

Peak undershoot = 380 -319.86 = 60.1 V

Settling time:

$$t_{settling} = t_s - t_0$$

From the table data voltage enters the 2%-5% range around settling time = 0.4 seconds.

Maximum Peak overshoot

$$\text{Maximum Peak overshoot (\%)} = \frac{Peak\ overshoot}{steady\ state\ voltage} \times 100$$

$$\text{Maximum Peak overshoot (\%)} = \frac{45\ V}{361\ V} \times 100 = 18.46\%$$

Voltage deviation (4 sec):

Voltage deviation = Excepted steady state voltage – Actual steady state voltage

Voltage deviation = 319.77 V – 361V = 41.23 V

Table 4. 8 Dynamic Response Analysis for Case 2

Parameters	Range
Peak overshoot voltage	45.02 V (0.5 sec)
Peak undershoot voltage	60.1V (4 sec)
Steady-state voltage	358.77V
Settling time	0.4 sec
Maximum Peak overshoot ($\% M_P$)	18.46 %
Voltage deviation (ΔV)	41.23V
Battery response time	**0.5 sec**

4.6.3 Case:3 Power management in DC Microgrid with HESS

- $\boldsymbol{P_{pv} + P_{Bat\_} + P_{SC\_} < P_{load}}$
- $\boldsymbol{P_{pv} + P_{Bat_{++}} + P_{SC_{++}} > P_{load}}$

In this case, When the power from photovoltaic ($\boldsymbol{P_{pv}}$) and the battery discharge ($\boldsymbol{P_{Bat\_}}$) is insufficient or during periods of rapid variation in power demand, the secondary source ($\boldsymbol{P_{SC\_}}$) acts as a short-term backup to support the load ($\boldsymbol{P_{load}}$). Conversely, when the load demand ($\boldsymbol{P_{load}}$) is less than the photovoltaic power generation ($\boldsymbol{P_{pv}}$), the surplus energy is allocated to charge the battery ($\boldsymbol{P_{Bat_{++}}}$) and the secondary source ($\boldsymbol{P_{SC_{++}}}$), optimizing energy management and ensuring efficient system operation.

Such scenarios commonly arise on partly cloudy days in the spring or summer, when intermittent cloud cover causes fluctuations in solar irradiance. These conditions result in inconsistent PV power generation, while high daytime loads, such as air conditioning, cooling systems, and industrial processes, introduce significant demand changes. The hybrid energy storage system (HESS) plays a critical role in addressing these challenges by dynamically balancing supply and demand, ensuring the uninterrupted operation of the DC microgrid.

The HESS achieves this balance by leveraging the complementary characteristics of its components. The supercapacitor, with its high-power density and rapid response time, efficiently handles transient power demands, such as sudden load increases or PV output drops due to shading.

This prevents voltage instability and minimizes disruptions. Simultaneously, the battery, characterized by higher energy density and longer discharge durations, provides sustained support during extended periods of reduced PV output, such as prolonged cloud cover or night-time. By integrating these two storage technologies, the HESS ensures smooth operation, reduces reliance on external power sources, and extends the lifespan of individual storage components by distributing the workload effectively. Figure 4.21 and Figure 4.22 represent the power management and Dynamic response anlysis for case 3.

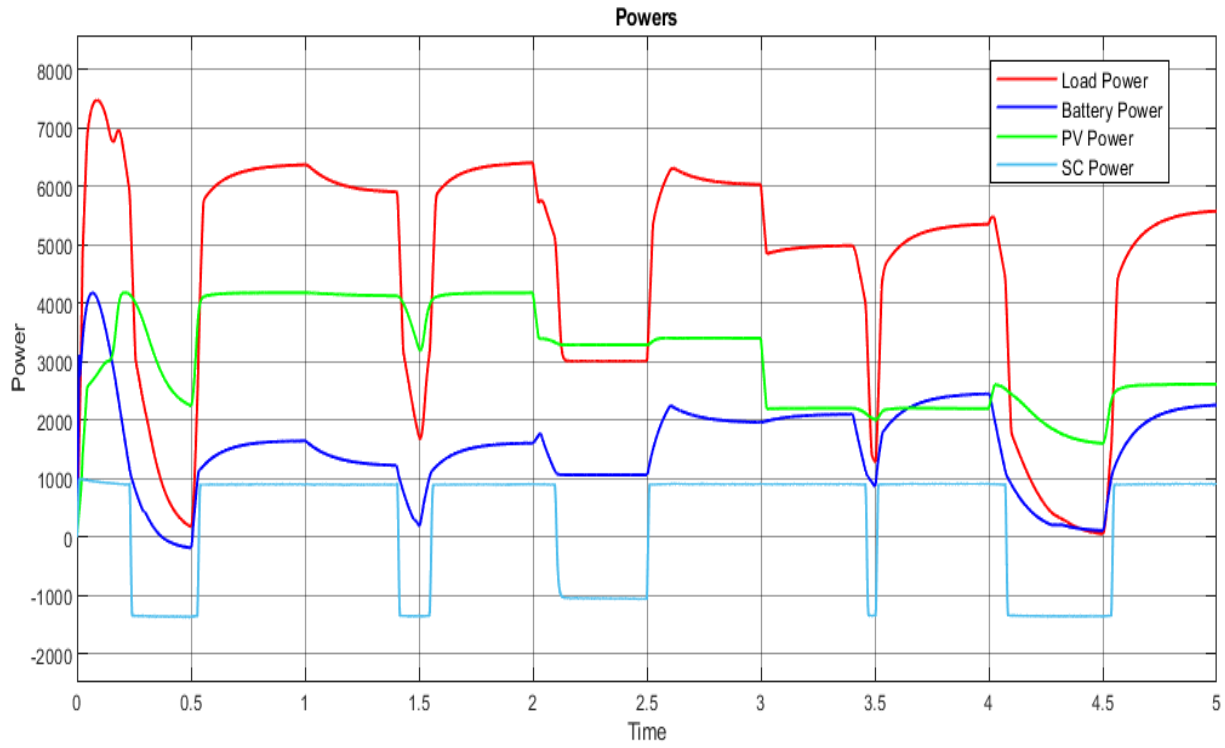

Figure 4. 21 Power Management for Case 3

The load power fluctuates significantly, ranging from as low as 53 W at 4.5 seconds to a peak of 6404 W at 2 seconds. The PV system provides a relatively stable power output, typically between 2000 W and 4000 W, acting as the primary energy source for meeting the base load. However, due to its slow dynamics, the PV system alone cannot handle transient load changes, necessitating the coordinated response of the battery and SC in the HESS.

The battery, with a response time of a few milliseconds, handles medium- to long-term power variations by either supplying or absorbing power as required. For instance, during a steady-state condition at 1.5 seconds (load power = 1713 W), the battery supplies 191.1 W to meet the demand, while the SC remains relatively inactive. The SC, with a significantly faster response time of 0.02 seconds, reacts instantly to sharp transients. In this case, at 0.5 seconds, during a sudden drop in load power, the SC discharges -1374.3 W almost immediately to stabilize the system, while the battery adjusts more gradually.

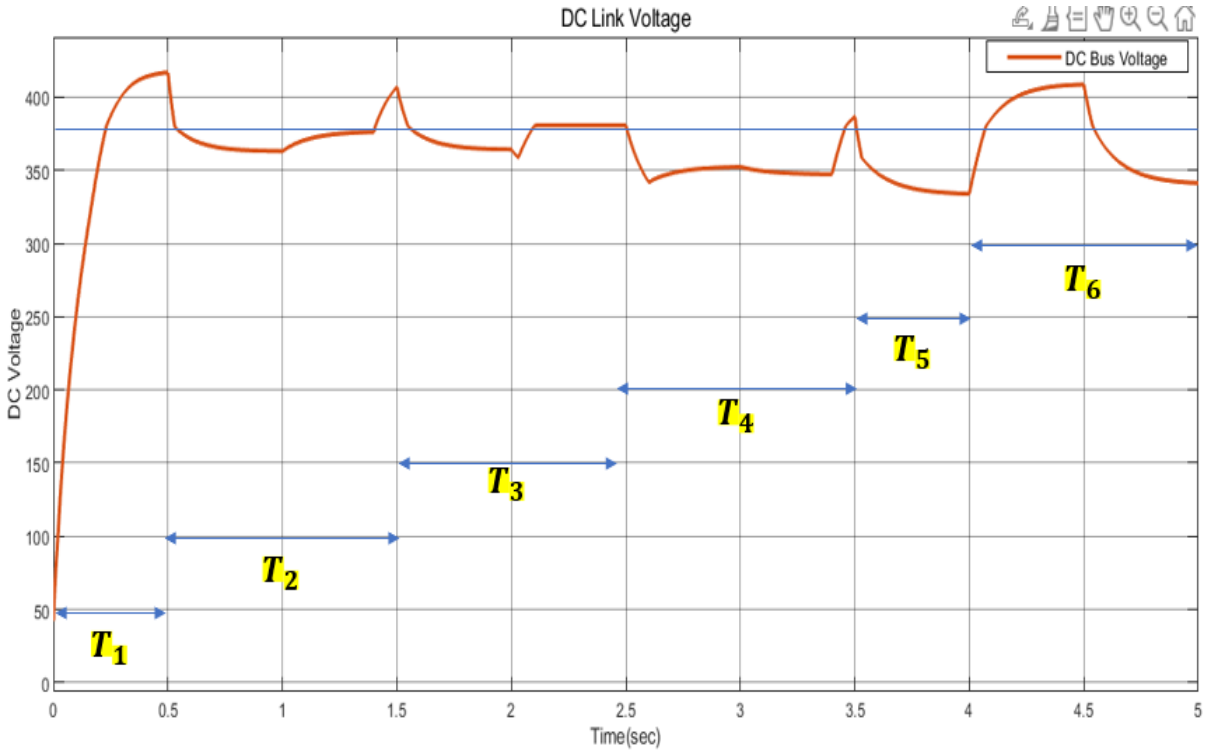

Figure 4. 22 Dynamic Response Analysis of DC Link Voltage for Case 3

During periods of higher and more dynamic load changes, both the battery and the supercapacitor (SC) work together. At 2 seconds (load power = 6404 W), the battery supplies 1606 W, providing sustained support, while the SC contributes 906.9 W, addressing the immediate transient. Similarly, at 1 second (load power = 6368 W), the battery delivers 1643 W, and the SC provides 891.6 W, showcasing their combined ability to manage rapid load increases. This coordinated response ensures system stability during such fluctuations.

Figure 4.22 shows the DC link voltage remains stable within a range of approximately 333 V to 417 V, despite varying load conditions. During high load scenarios, such as at 1 second (load power = 6368 W), the voltage dips to 363.12 V but recovers quickly. Similarly, at 4 seconds (load power = 5353 W), the voltage decreases to 333.9 V but remains within acceptable limits. During lower load conditions, such as at 4.5 seconds (load power = 53 W), the voltage rises to 408.6 V, highlighting the system's ability to stabilize effectively. Figure 4.23 shows the State of charge of the battery and Figure 4.24 shows the State of charge of the Supercapacitor for case 3. The battery and supercapacitor alternate between charging and discharging as needed, with the battery efficiently managing the energy balance while the supercapacitor supports the system by rapidly supplying or absorbing energy, depending on the load's demands. Table 4.9 shows the Parameters for Power Management with Battery Case 3

Table 4. 9 Parameters for Power Management with Battery Case 3

Time	Load Power (W)	PV Power (W)	Battery Power (W)	SC Power (W)	DC link voltage(V)
0.5	170.2	2244.1	-187.9	-1374.3	416.9
1	6368	4178.7	1643	891.6	363.12
1.5	1713	3215	191.1	-1352	407
2	6404	4177	1606	906.9	364.2
2.5	3010	3288	1064	-1056	380.8
3	6029	3402	1960	893.6	352.3
3.5	1286	2007	866.5	-1349	386.8
4	5353	2196	2451	900	333.9
4.5	53	1601	109.5	-1370	408.6
5	5576	2615	2257	909	341.3

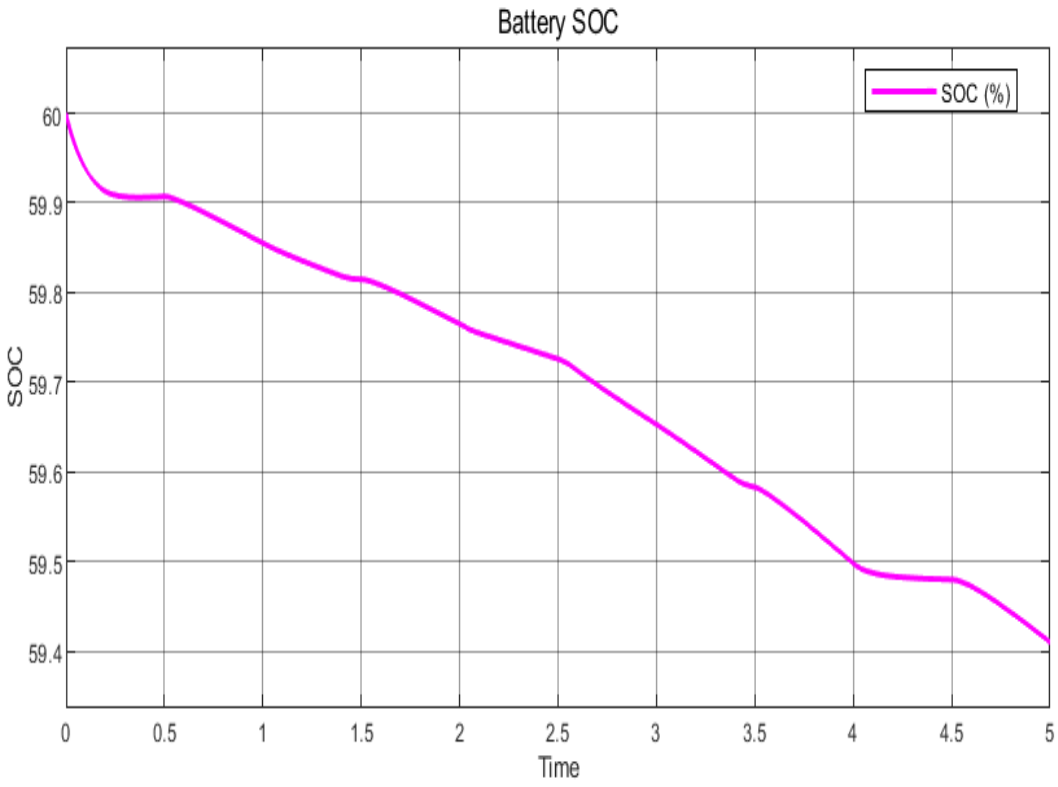

Figure 4. 23 Battery SOC

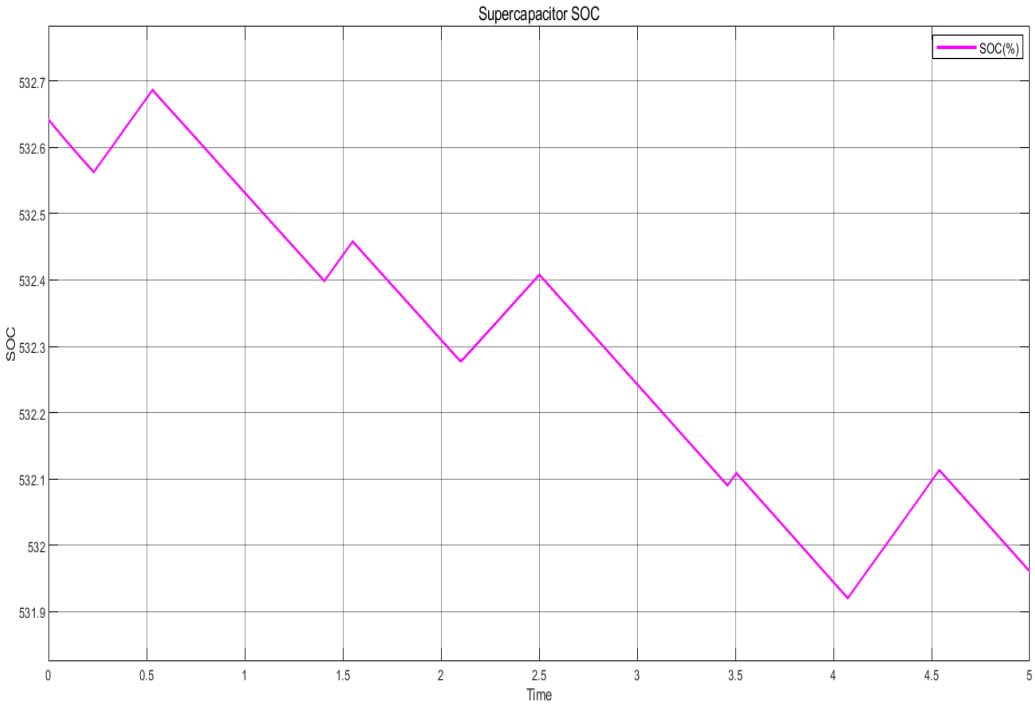

Figure 4. 24 SC SOC

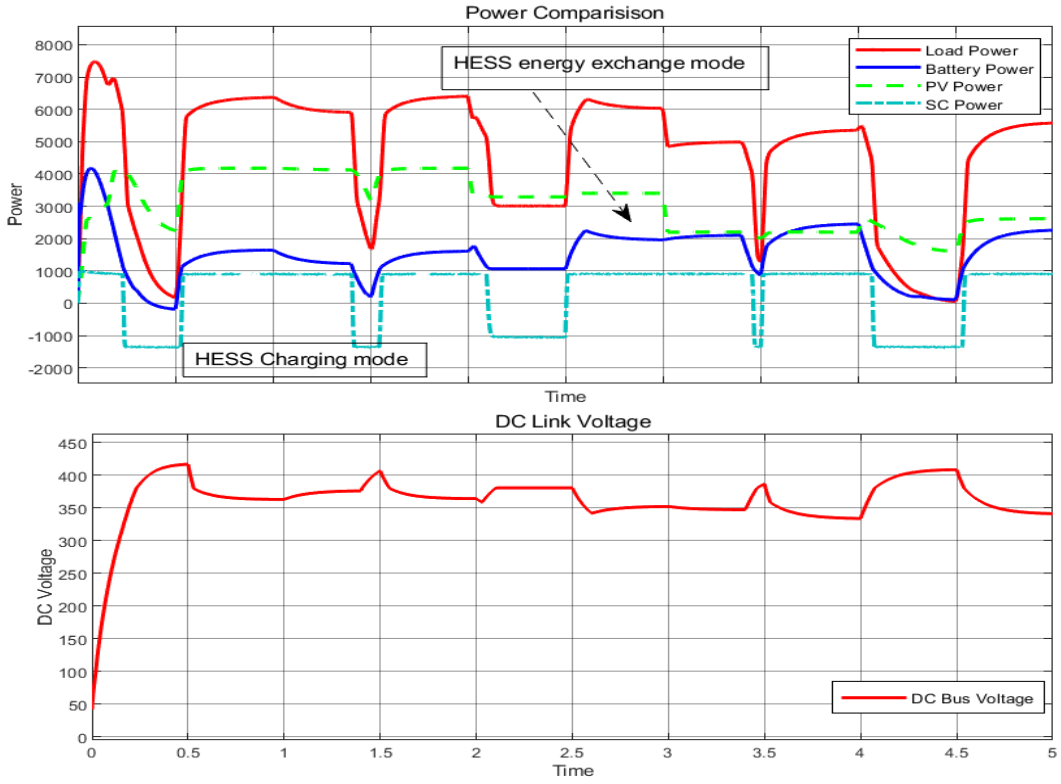

Figure 4. 25 Power Output and DC Link Voltage Profile for Case 3

Figure 4.25 represents the analysis of the dynamic response in a DC microgrid. Therefore, Calculate the system's dynamic response concerning key performance metrics, such as peak overshoot, peak undershoot, settling time, steady-state voltage, and voltage deviation.

Peak Overshoot:

$$V_{overshoot} = maxV_{dc}(t), for t > t_0$$

$$V_{overshoot} = 416.9\,V(0.5sec)$$

Steady-state voltage = 390.6 V

Peak overshoot = 416.9 – 390.6 = 36 V

Peak Undershoot:

$$V_{undershoot} = min\{V_{dc}(t)\}, for\ t > t_0$$

Peak undershoot occurs at time 4 sec with a voltage of 379 V.

Peak undershoot = 390.6 – 379 = 11.6 V

Settling time:

$$t_{settling} = t_s - t_0$$

settling time = 0.2 sec

Maximum Peak overshoot

$$\text{Maximum Peak overshoot (\%)} = \frac{Peak\ overshoot}{steady\ state\ voltage} \times 100$$

$$\text{Maximum Peak overshoot (\%)} = \frac{36\,V}{390.6\,V} \times 100 = \mathbf{6.5\%}$$

Voltage deviation:

Voltage deviation = Excepted steady state voltage – Actual steady state voltage

Voltage deviation = 350V – 390.6 V = 40.6 Vs

Here, Table 4.10 represents the parameters of dynamic response analysis for case 3

Table 4. 10 Dynamic Response Analysis for Case 3

Parameters	Range
Peak overshoot voltage	36 V (0.5 sec)
Peak undershoot voltage	11.6 V (4 sec)
Steady-state voltage	390.6 V
Settling time	0.2 sec
(% M_P) Maximum Peak overshoot	6.5%
(ΔV) Voltage deviation	40.6 V
Battery response time	0.1 sec
SC response time	0.01 ec

4.6.4 Case:4 Power management in DC Microgrid with Fuel cell (Stand by)

$$\boldsymbol{P_{pv}} = 0 \; or \; Minimum \, , \;\; \boldsymbol{P_{Bat\_} + P_{sc\_} + P_{FC\_} < P_{load}}$$

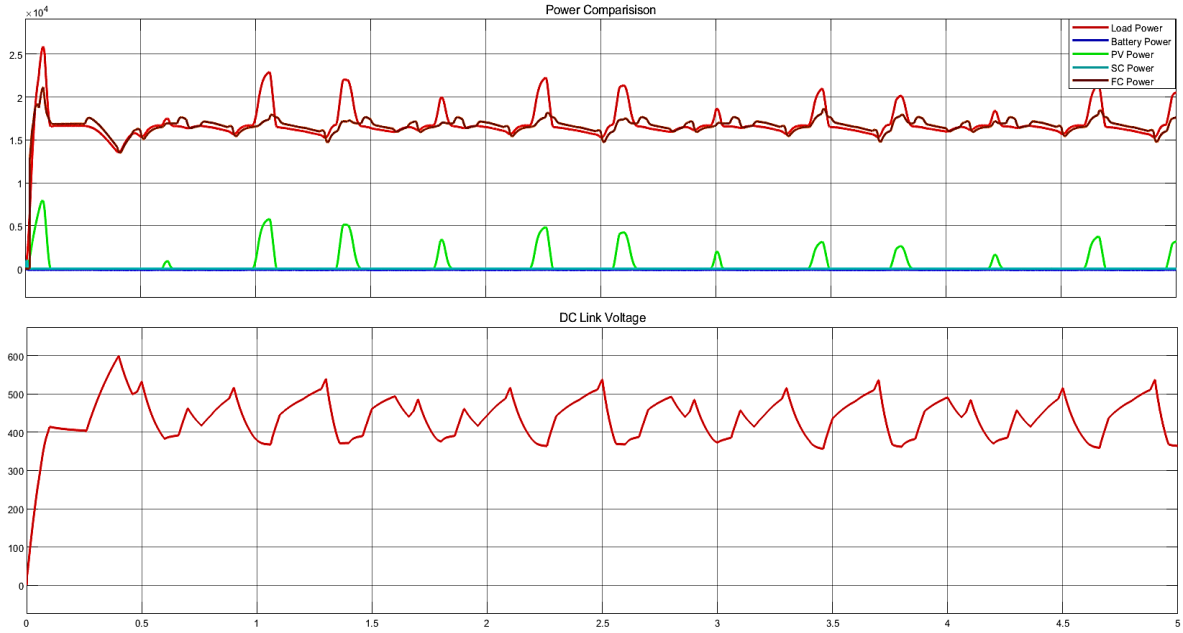

Figure 4. 26 Power management and DC link bus for case 4

Figure 4.26 illustrates the operation of a DC microgrid where the fuel cell functions as a standby power source. In this case, the fuel cell remains inactive under normal operating conditions, only activating during emergencies or when other power sources are insufficient to meet the load demand. This strategy allows the system to optimize the use of renewable and stored energy while keeping the fuel cell as a backup to enhance reliability and reduce dependency on fossil fuels.

The DC microgrid effectively prioritizes other sources, such as the battery, which serves as the primary energy buffer by dynamically adjusting to variations in load demand. The battery responds to both short-term fluctuations and longer-term energy storage requirements, providing a consistent power supply even when photovoltaic generation is intermittent or during higher load periods. A supercapacitor (SC) is utilized to handle transient spikes and sudden changes in power requirements. Its rapid response to fast load changes ensures the system remains stable, protecting sensitive electronic devices from voltage instability or surges. The SC effectively smooths out these rapid power fluctuations, preventing undue stress on other energy storage components.

Meanwhile, the photovoltaic (PV) system provides a steady and consistent contribution to the overall energy supply, especially during daylight hours. It harnesses solar energy, reducing reliance on non-renewable sources, and helps offset the energy required from the battery and fuel cell. This renewable integration is central to the microgrid's sustainability, ensuring that energy demand is met efficiently while lowering environmental impact.

The voltage exhibits periodic fluctuations between 0 and 5 seconds, correlating with changes in load demand. These oscillations are particularly notable during the initial 0.5 seconds, where the system experiences rapid changes due to transient effects as the energy sources respond to load dynamics. During this period, the supercapacitor quickly compensates for these brief spikes, while the battery gradually adjusts its output. After this initial period, the voltage fluctuations stabilize, maintaining an average value despite occasional peaks and dips caused by variations in load or the response of the energy storage components. The system’s design ensures that these fluctuations are minimized, maintaining operational efficiency and reducing wear and tear on components.

The stable behavior of the DC link voltage reflects effective regulation and coordination among the energy sources, which communicate to balance the power supply with load demand in real time. This dynamic response mechanism is key to ensuring the DC microgrid can continue to

operate reliably under normal conditions. While the fuel cell remains in standby mode, it is always ready to provide additional power when needed, for example, during periods of high demand or in the event of other system failures.

This operational strategy ensures the DC microgrid functions seamlessly, even under changing environmental conditions or unexpected spikes in demand. By maintaining optimal control of its energy sources, the system maximizes efficiency and enhances overall system resilience. The DC microgrid design also reduces the need for constant external grid reliance, providing both operational independence and long-term sustainability.

4.7 Comparative Performance Evaluation

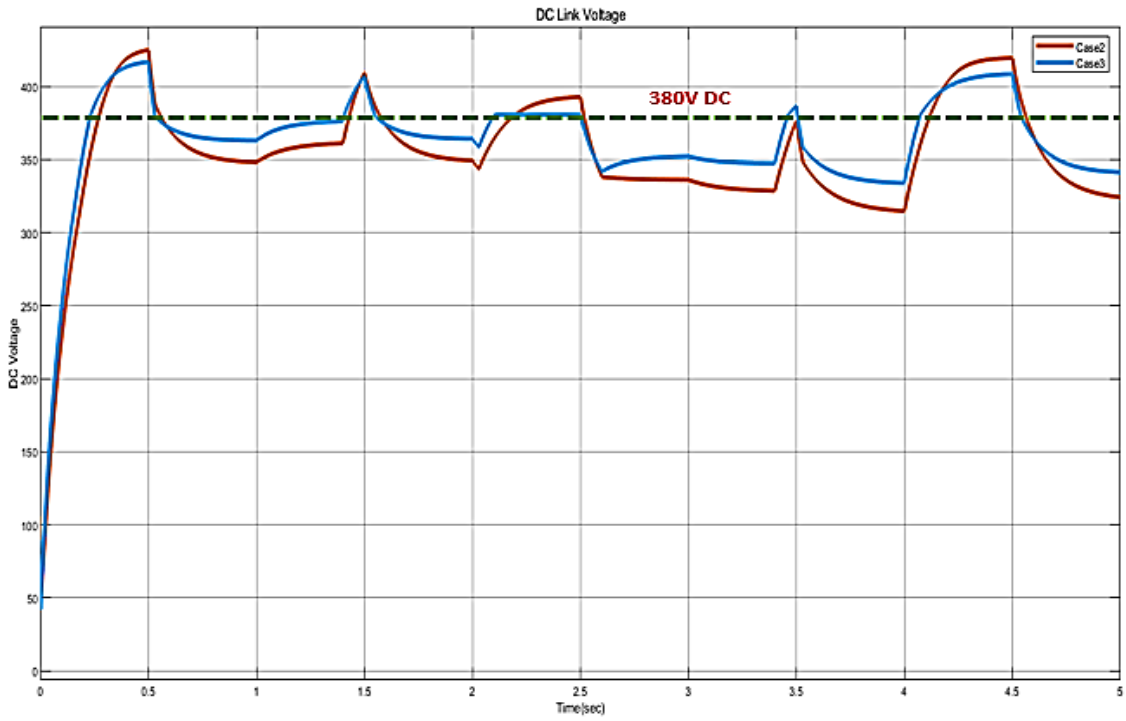

Figure 4. 27 Performance comparison of Cases 1, 2, and 3 in a DC microgrid

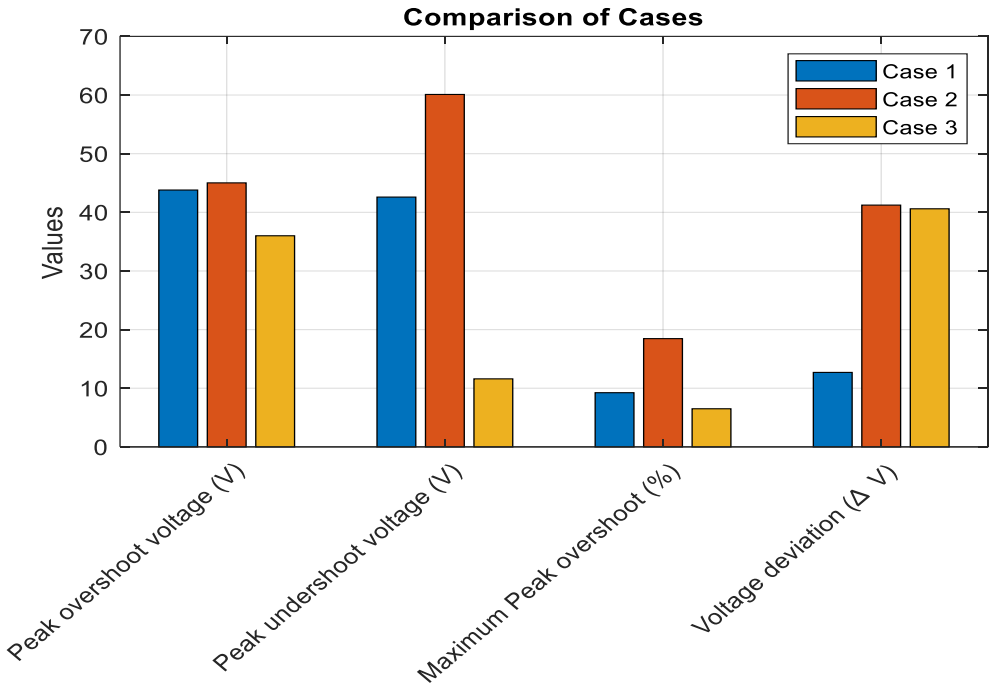

Figure 4. 28 Comparison of all parameters for cases 1,2 and 3

Figures 4.27 and 4.28 represent the comparative analysis of the three cases for voltage regulation and transient response in a DC microgrid. Table 4.11 shows the parameters of all three cases.

Table 4. 11 Parameters comparison of all cases

Parameters	**Case:1**	**Case:2**	**Case:3**
Peak overshoot voltage	43.8 V (2.5 sec)	45.02 V (0.5 sec)	**36 V** (0.5 sec)
Peak undershoot voltage	42.6V (3.5 sec)	60.1V (4 sec)	**11.6V** (4 sec)
Settling time (t_s)	0.5 sec	0.4 sec	**0.2 sec**
Maximum Peak overshoot (% M_P)	9.24%	18.46 %	6.5 %
(ΔV) Voltage deviation	12.7V	41.23V	40.6V
Battery response time	--	0.5 sec	**0.1 sec**
SC response time	--	--	**0.01 sec**

Summary

Case 1 exhibits slower stabilization dynamics with moderate voltage regulation capabilities. It achieves the lowest voltage deviation but suffers from a prolonged settling time of 0.5 seconds and lacks the integration of fast-response energy storage systems, making it less effective in handling transient disturbances.

Case 2 improves stabilization dynamics with a settling time of 0.4 seconds and introduces a battery response time of 0.5 seconds. However, it struggles with significant voltage overshoots (45.02 V) and undershoots (60.1 V), resulting in higher voltage instability and a maximum peak overshoot percentage of 18.46%. This limits its effectiveness in maintaining precise voltage regulation during dynamic conditions.

Case 3 achieves the most optimal performance by integrating a hybrid energy storage system (HESS) consisting of a battery and supercapacitor. This configuration enables rapid transient response, with a battery response time of 0.1 seconds and a supercapacitor response time of 0.01 seconds. Case 3 minimizes voltage overshoot (36 V) and undershoot (11.6 V), achieves the fastest settling time (0.2 seconds), and reduces the maximum peak overshoot percentage to 6.5%. This demonstrates significant improvement in voltage stability.

Case 3 effectively meets the objective of minimizing response time by leveraging the supercapacitor's ultra-fast response and the battery's moderate response, ensuring efficient voltage stability. This demonstrates the importance of Hybrid Energy Storage Systems (HESS) in achieving high-speed dynamic stabilization. The combination of both energy storage elements ensures reliable and efficient operation in DC microgrids, highlighting the critical role of advanced systems for optimal performance. Case 3 effectively minimizes response time but requires a further reduction in settling time and overshoot to enhance system performance. The integration of the supercapacitor's ultra-fast response and the battery's moderate response plays a key role in voltage stability, but optimizing their coordination can lead to quicker stabilization. Optimization is used to fine-tune the parameters of the Hybrid Energy Storage System (HESS), ensuring that both the supercapacitor and battery work together more efficiently. This helps minimize overshoot, reduce settling time, and improve dynamic response, ultimately ensuring more precise, reliable, and efficient operation in Island DC microgrids.